INL/CON-20-60255-Revision-0

Cumulative short-lived photofission product yields for nuclear forensic application

July 2021

Ariana A Foley, Haori Yang

Changing the World's Energy Future

INL is a U.S. Department of Energy National Laboratory operated by Battelle Energy Alliance, LLC

INL/CON-20-60255-Revision-0

Cumulative short-lived photofission product yields for nuclear forensic application

Ariana A Foley, Haori Yang

July 2021

Idaho National Laboratory
Idaho Falls, Idaho 83415

http://www.inl.gov

Prepared for the
U.S. Department of Energy
Under DOE Idaho Operations Office
Contract DE-AC07-05ID14517

ANS Virtual Winter Meeting

Nuclear is good for you.

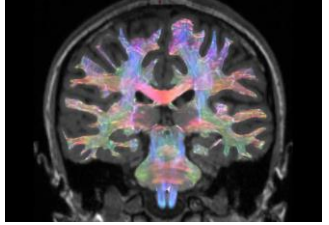






Cumulative short-lived photofission product yields for nuclear forensic application




Ari Foley[1,2] and Haori Yang[2]

[1] Idaho National Laboratory, Idaho Falls, ID 83415

[2] School of Nuclear Science & Engineering, Oregon State University, Corvallis, OR 97333

INL/CON-20-60255

Idaho National Laboratory

Oregon State University

Introduction

- In post-detonation nuclear forensics, FPY distribution could **give indication to the neutron energy spectrum** that had induced fission
- Photon-induced fission, "**photofission**", is most probable at GDR and the resulting FPY distribution around this energy **closely resembles that of DT neutron fission**

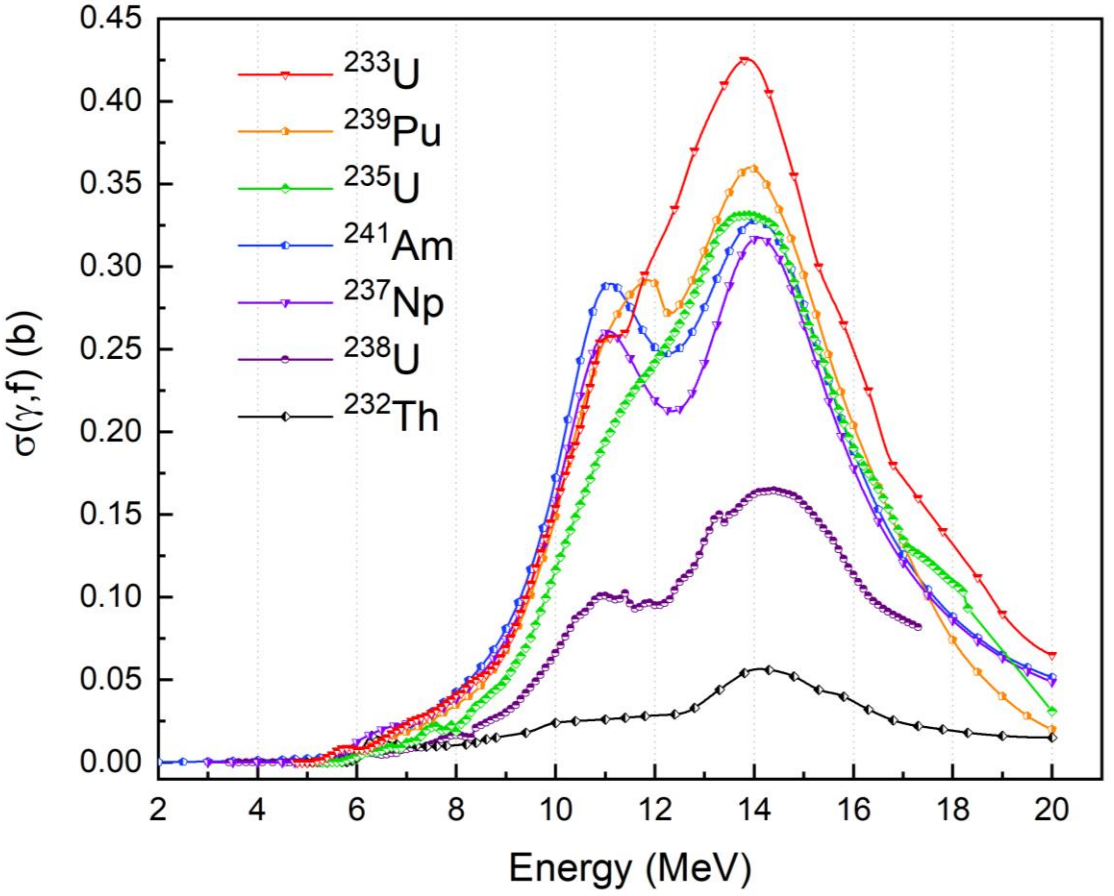

[1] ENDF-B/VII.0: Accessed from Janis 4.0, Nuclear Energy Agency, Organization for Economic Co-operation and Development. https://www.oecd-nea.org/janis/

Motivation

- **Improving nuclear data**
  - Photonuclear data heavily reliant on nuclear models; limited experimental data often inconsistent
- **New and improved isotope production** for isotopes of interest to nuclear forensics
  - Less costly and more flexible method to benefit nuclear forensics exercises allowing analysis techniques to be tested

Objectives

1. **Measure short lived ($T_{1/2}$≤50s) photofission product yields** for ^{238}U and ^{232}Th at 8, 14, and 20 MeV endpoint energies
2. **Perform thorough uncertainty analysis** to ensure uncertainty can be confidently declared
3. **Develop experimental and analysis methods** for consistent future photofission product yield measurements of additional fissional nuclides and endpoint energies

Fission Product Yield Distributions

- Distribution of fission products dependent on several factors; most strongly target nucleus and excitation energy
- In the multimode-fission model, FPY mass distribution is understood by the sum of multiple fission modes
- Symmetric superlong mode (SL), and two asymmetric modes standard I (STI) and standard II (STII) for 3 mode fit (5 Gaussians)

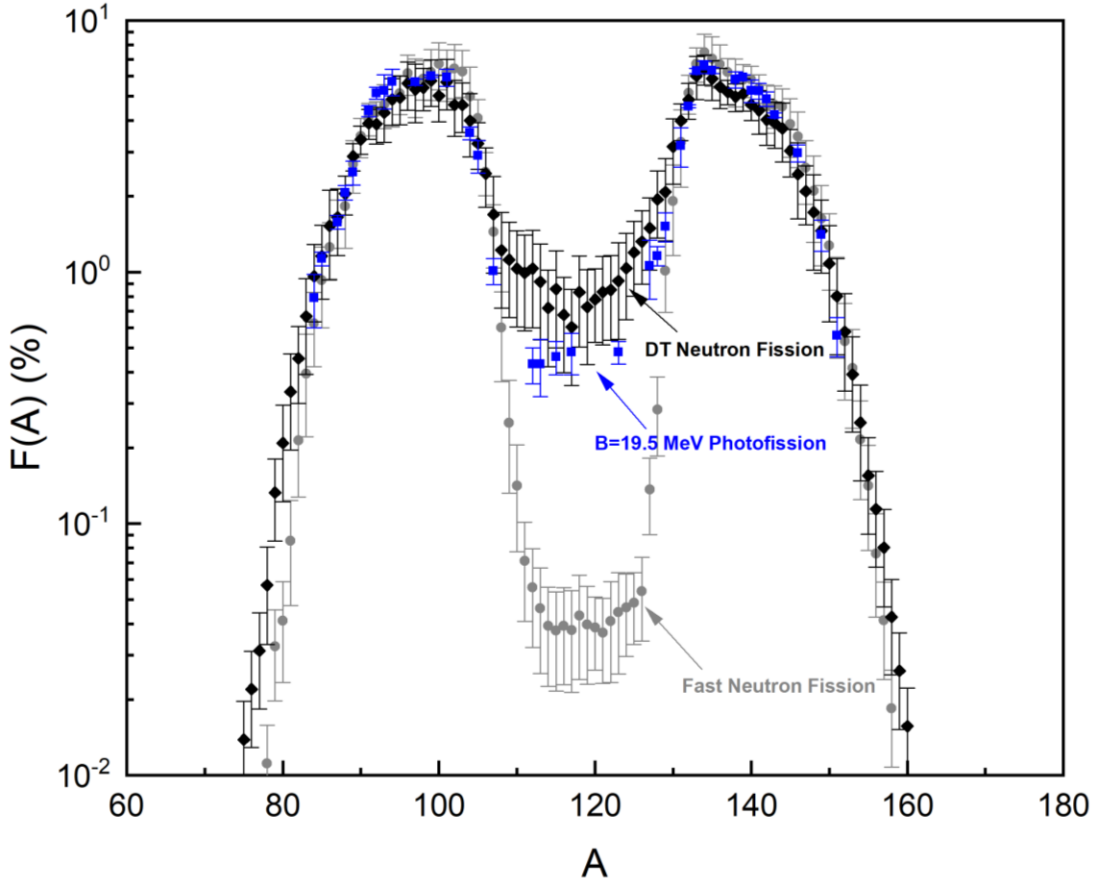

$$Y(A) = K_{SL} \cdot e^{-\frac{(A-\bar{A}_{SL})^2}{2\sigma^2_{SL}}} + K_{STI} \cdot e^{-\frac{(A-\bar{A}_{SL}-D_{STI})^2}{2\sigma^2_{STI}}} + K_{STI} \cdot e^{-\frac{(A-\bar{A}_{SL}+D_{STI})^2}{2\sigma^2_{STI}}} + K_{STII} \cdot e^{-\frac{(A-\bar{A}_{SL}-D_{STII})^2}{2\sigma^2_{STII}}} + K_{STII} \cdot e^{-\frac{(A-\bar{A}_{SL}+D_{STII})^2}{2\sigma^2_{STII}}}$$

[1] ENDF-B/VII.0: Accessed from Janis 4.0, Nuclear Energy Agency, Organization for Economic Co-operation and Development. https://www.oecd-nea.org/janis/
[2] S.S. Beleshev et al. "Mass yield distributions and fission modes in photofission of ^{238}U below 20 MeV". Physical Review C 91, 034603 (2015)

Multimode Fission Model - ^{238}U

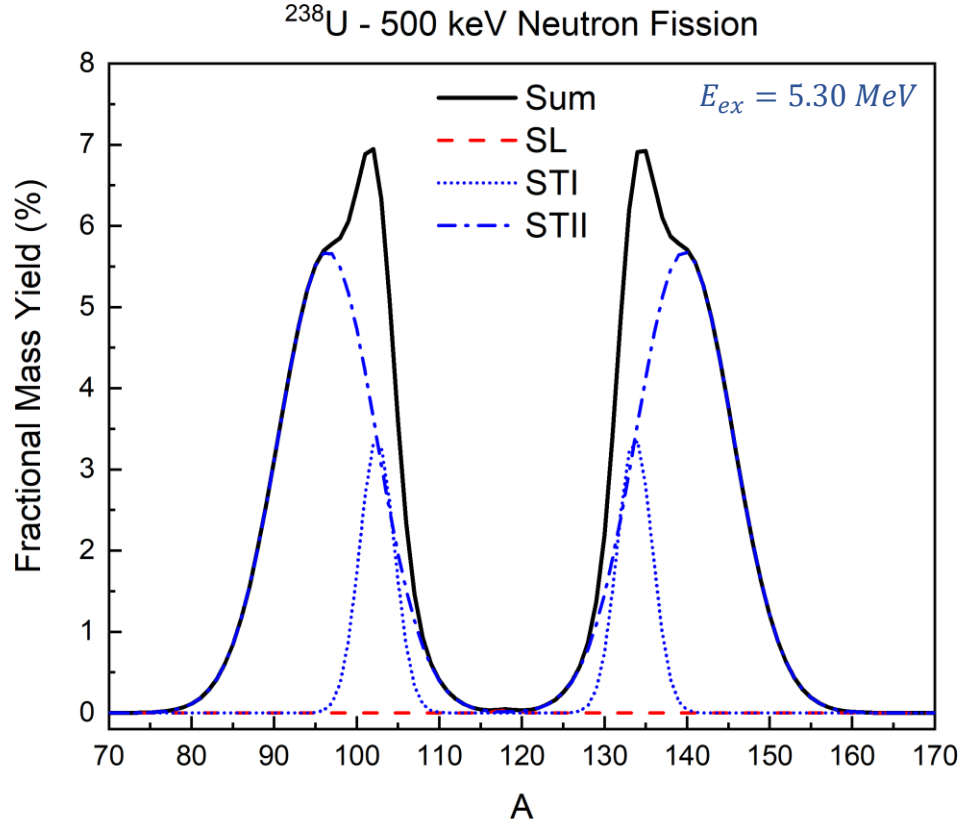

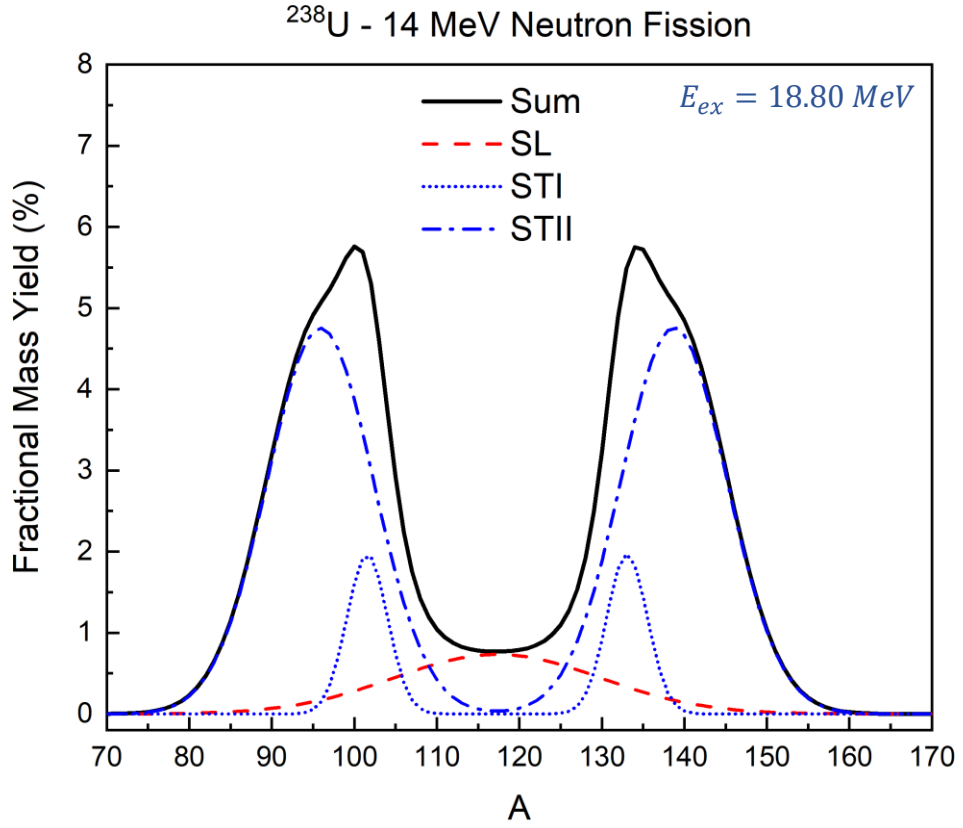

Neutron-induced fission for fast (500 keV) and DT (14 MeV) neutrons used as reference[1]

Symmetric SL mode increases at higher energies

Ratio between two asymmetric STI and STII modes of interest

[1] ENDF-B/VII.0: Accessed from Janis 4.0, Nuclear Energy Agency, Organization for Economic Co-operation and Development. https://www.oecd-nea.org/janis/

Multimode Fission Model - ^{232}Th

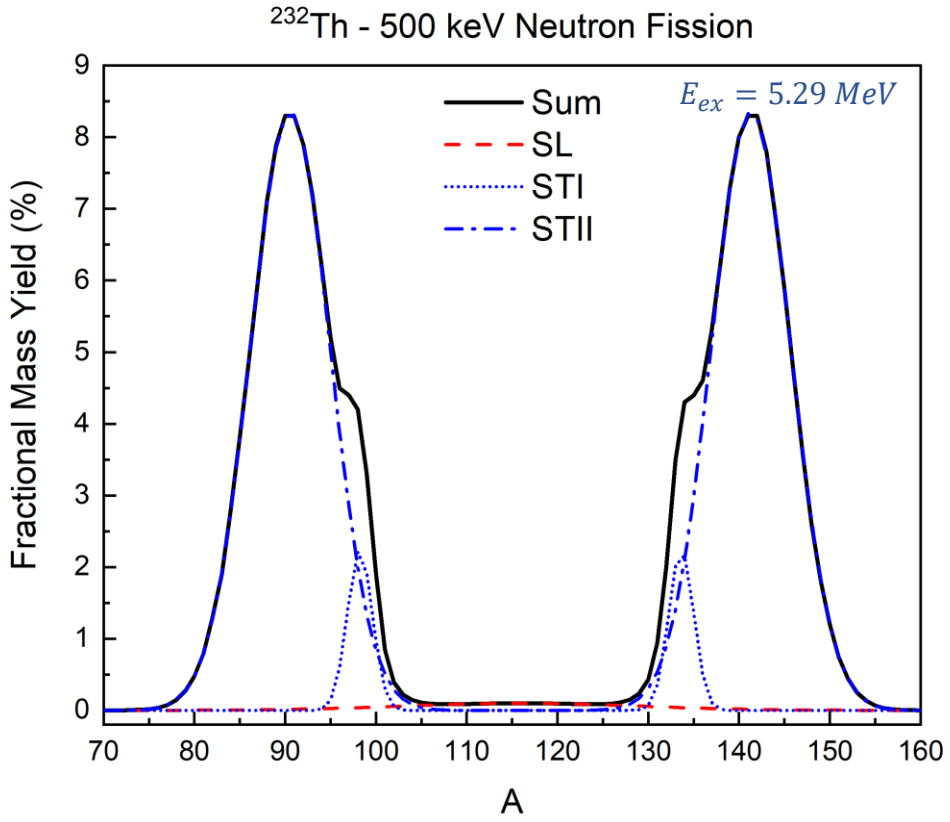

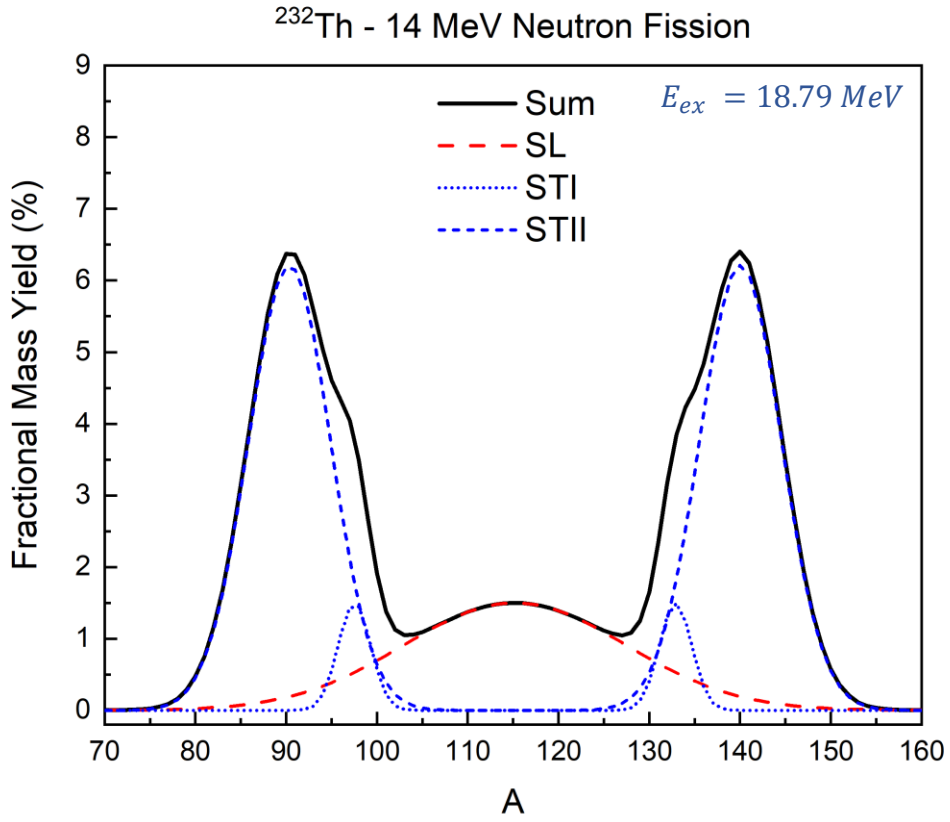

Neutron-induced fission for fast (500 keV) and DT (14 MeV) neutrons used as reference[1]

Third “peak” in valley

Symmetric SL mode increases at higher energies

Difference in two asymmetric STI and STII modes of interest

[1] ENDF-B/VII.0: Accessed from Janis 4.0, Nuclear Energy Agency, Organization for Economic Co-operation and Development. https://www.oecd-nea.org/janis/

Experimental Materials and Methods

Photonuclear Reactions

- **Yield of photonuclear reactions** calculated with bremsstrahlung X-ray flux and interaction cross sections[1] necessary to calculate

$$Y(B) = N_T \int_0^B \frac{\phi(B,E)}{dE} \cdot \sigma_{\gamma,f}(E) dE$$

- **Excitation energy of target nucleus** useful in comparing monoenergetic interaction with those produced with energy spectrum

$$\langle E^*(B) \rangle = \frac{\int_0^B \frac{\phi(B,E)}{dE} \cdot \sigma_{\gamma,f}(E) E dE}{\int_0^B \frac{\phi(B,E)}{dE} \cdot \sigma_{\gamma,f}(E) dE}$$

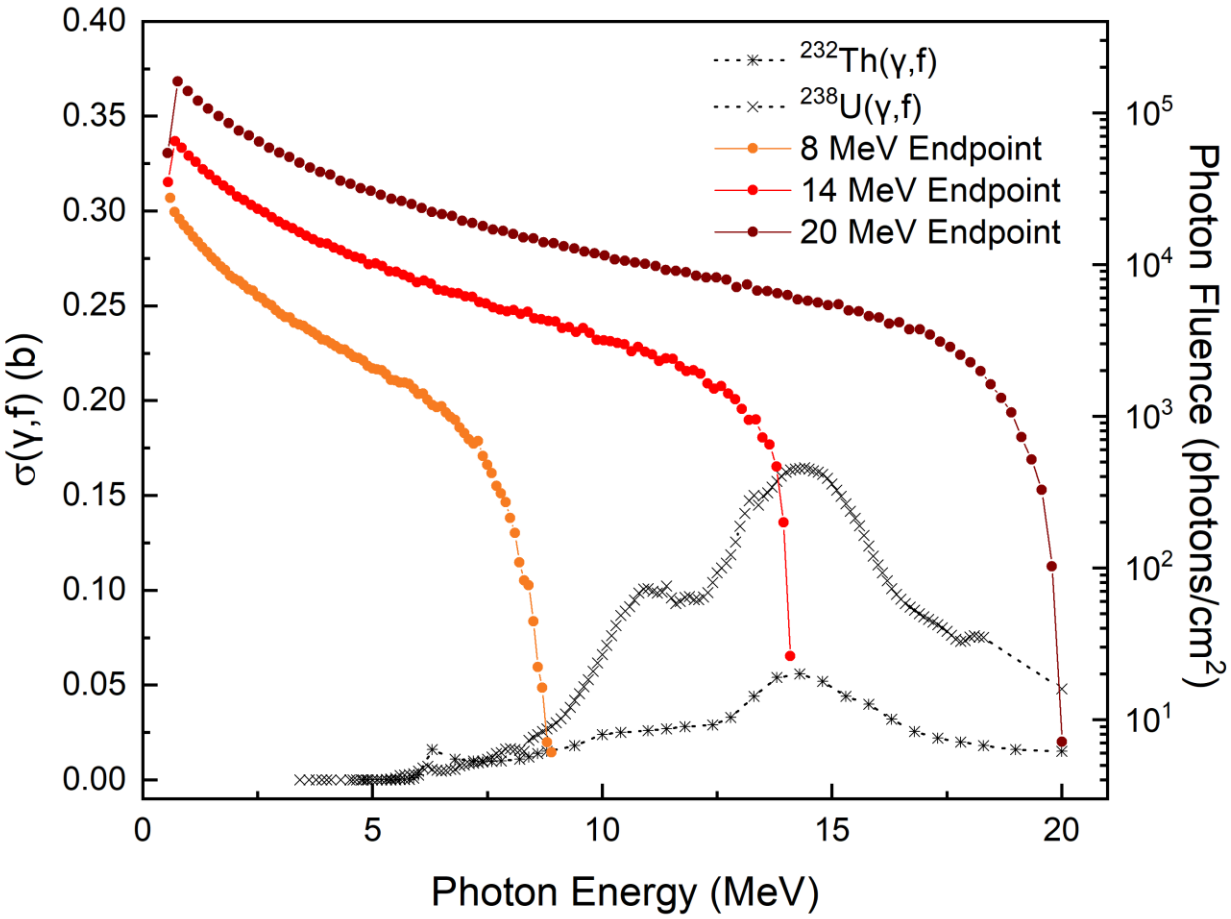

[1] ENDF-B/VII.0: Accessed from Janis 4.0, Nuclear Energy Agency, Organization for Economic Co-operation and Development. https://www.oecd-nea.org/janis/

Target Foils

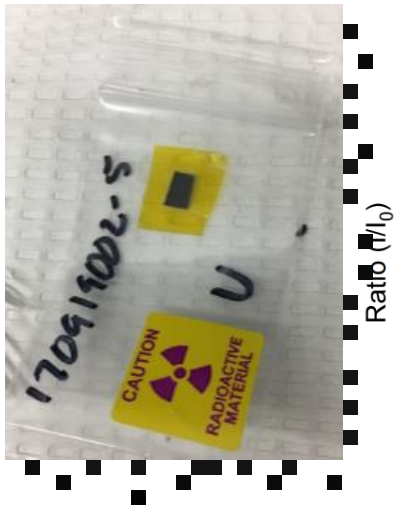

Uranium Foil Attenuation Fit

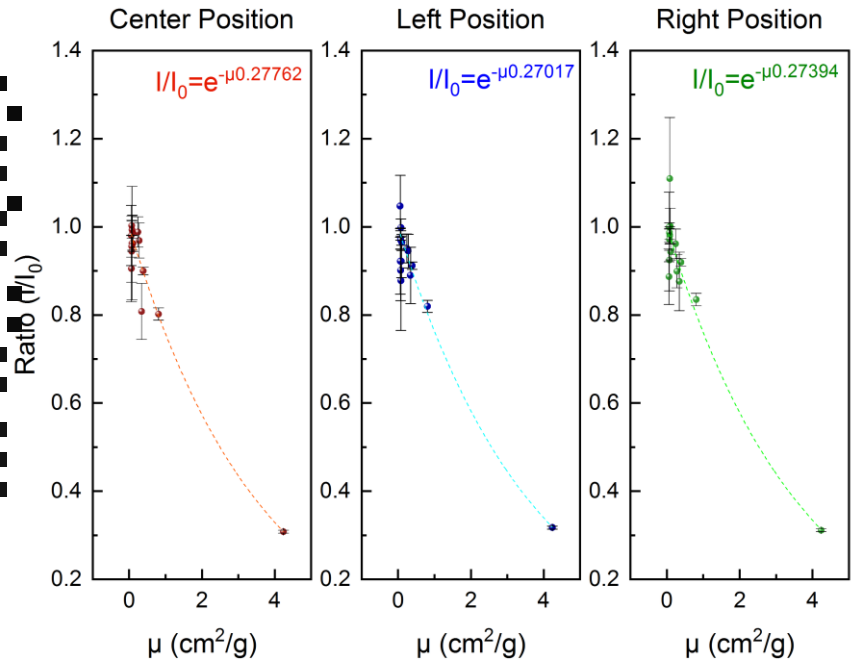

Thorium Foil Attenuation Fit

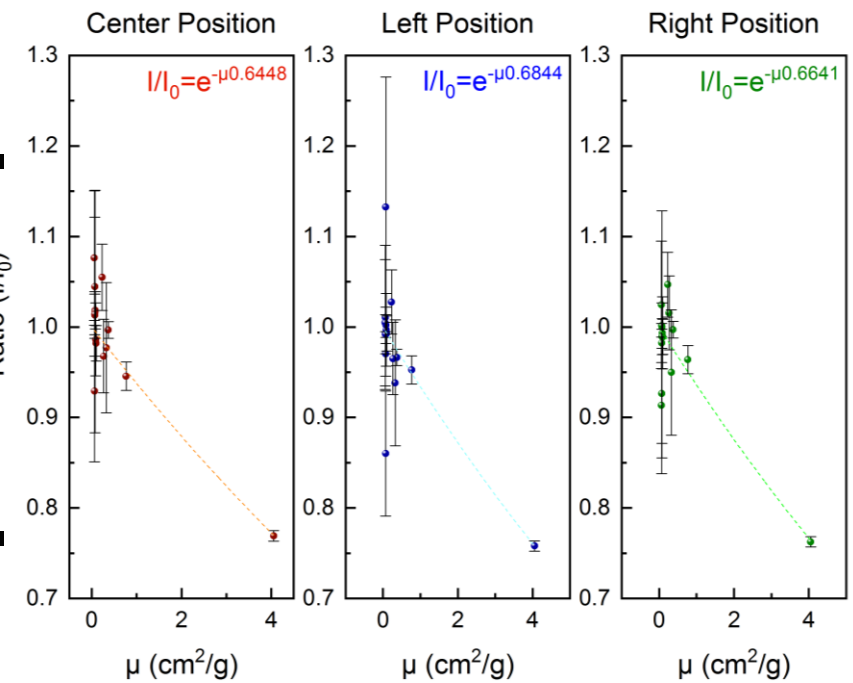

Mass and Geometry of Samples from Cycling Experiment

Nuclide	Endpoint Energy	Mass (g)	ρx ($\frac{g}{cm^2}$)	Thickness (mm)
^{238}U	8 MeV	0.1172	0.2739±0.0013	0.1445 ±0.0007
	14 MeV	0.1113		
	20 MeV	0.1133		
^{232}Th	8 MeV	0.1004	0.6644±0.0009	0.0567±0.0005
	14 MeV	0.1100		
	20 MeV	0.0990		

$$I/I_0 = e^{-\mu\rho x}$$

- Foil thickness calculated from ^{152}Eu γ-ray attenuation
- Attenuation data accessed from NIST XCOM[2]

[2] NIST Physical Measurement Laboratory, XCOM: Photon Cross Sections Database. https://www.nist.gov/pml/xcom-photon-cross-sections-database

ISU-IAC 25-MeV S-Band Linear Accelerator

- Experiments performed at the Idaho Accelerator Center (IAC)
- Adjusted Parameters
  - Endpoint Energy (B)
  - Repetition Rate (in Hz)
  - Pulse Width (in μs)
- Measured Parameters
  - Charge per pulse (nC)

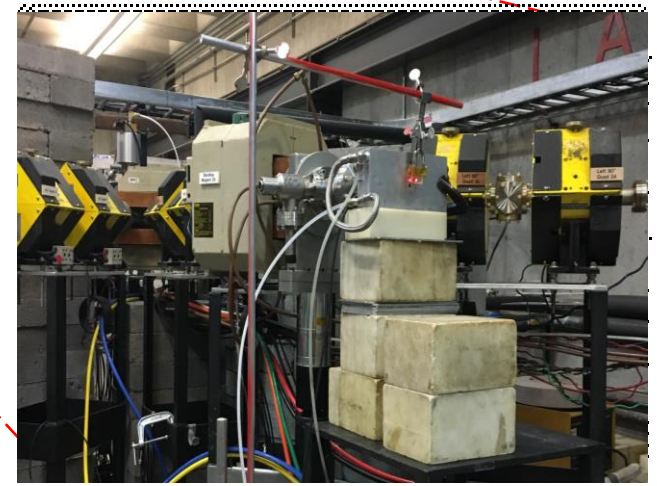

Linac Parameters from Cycling Experiment

Target	B (MeV)	$\langle E^*(B) \rangle$ (MeV)	$1/\tau$ (Hz)	Cycles	$Q_{Average}$ (nC)
^{238}U	8	6.78±0.01	200	50	361.39±2.88
^{238}U	14	10.30±0.01	15	50	186.73±1.26
^{238}U	20	12.59±0.01	2	50	302.42±1.20
^{232}Th	8	6.74±0.02	200	60	257.90±1.22
^{232}Th	14	9.22±0.01	30	60	190.01±1.35
^{232}Th	20	11.50±0.03	6	50	303.36±1.64

In-Hall Experimental Setup

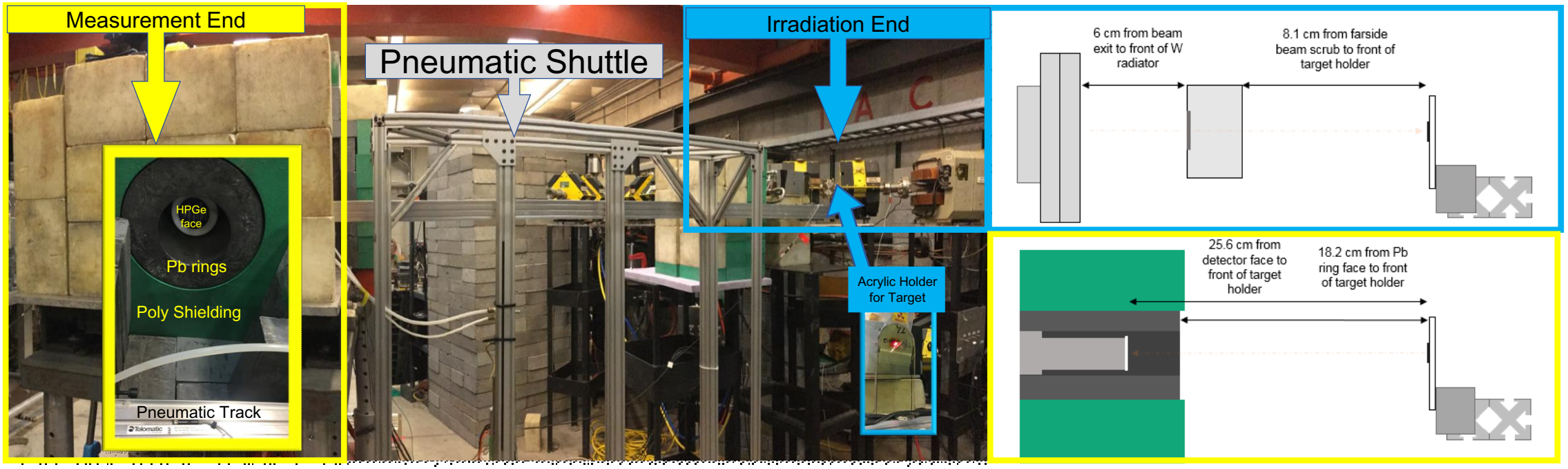

Simulation & Characterization

Electron Beam to Bremsstrahlung

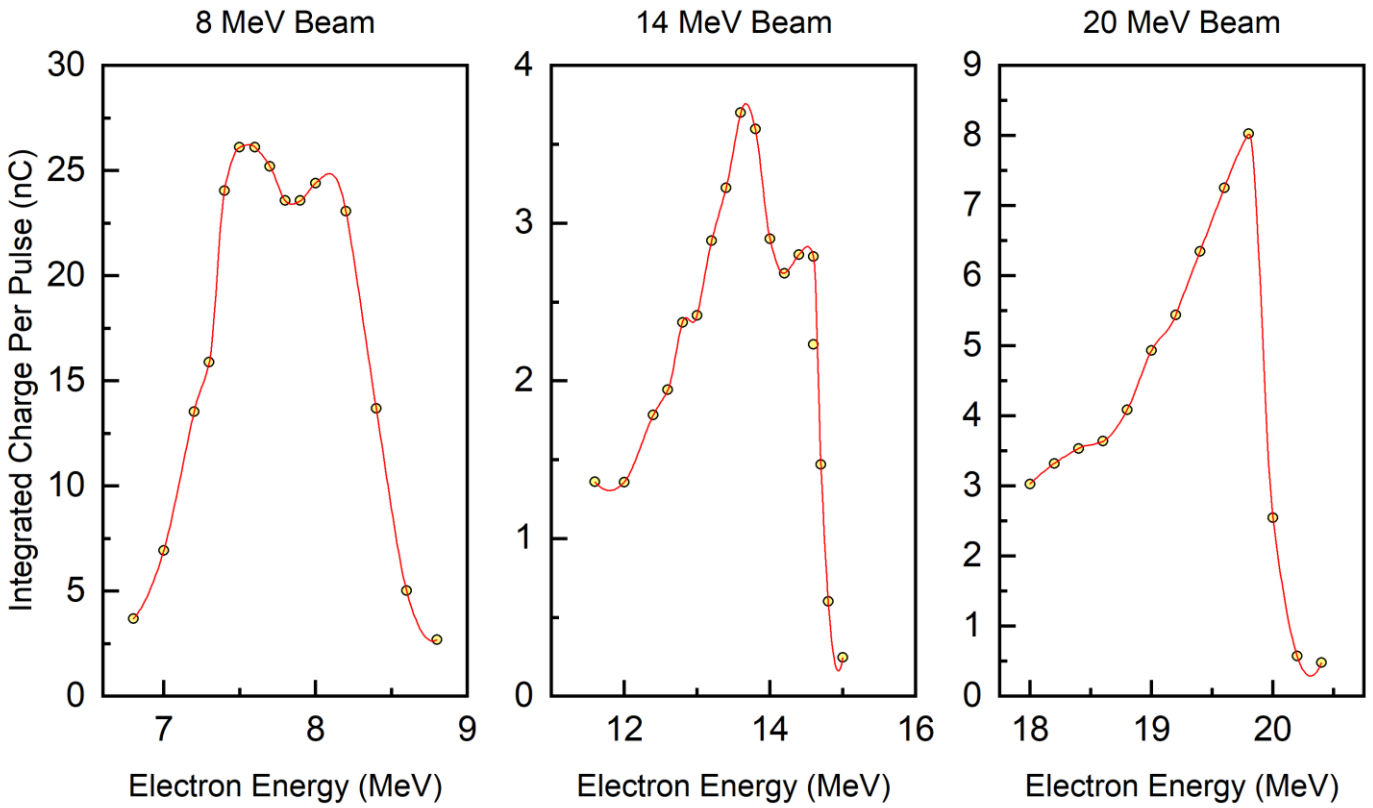

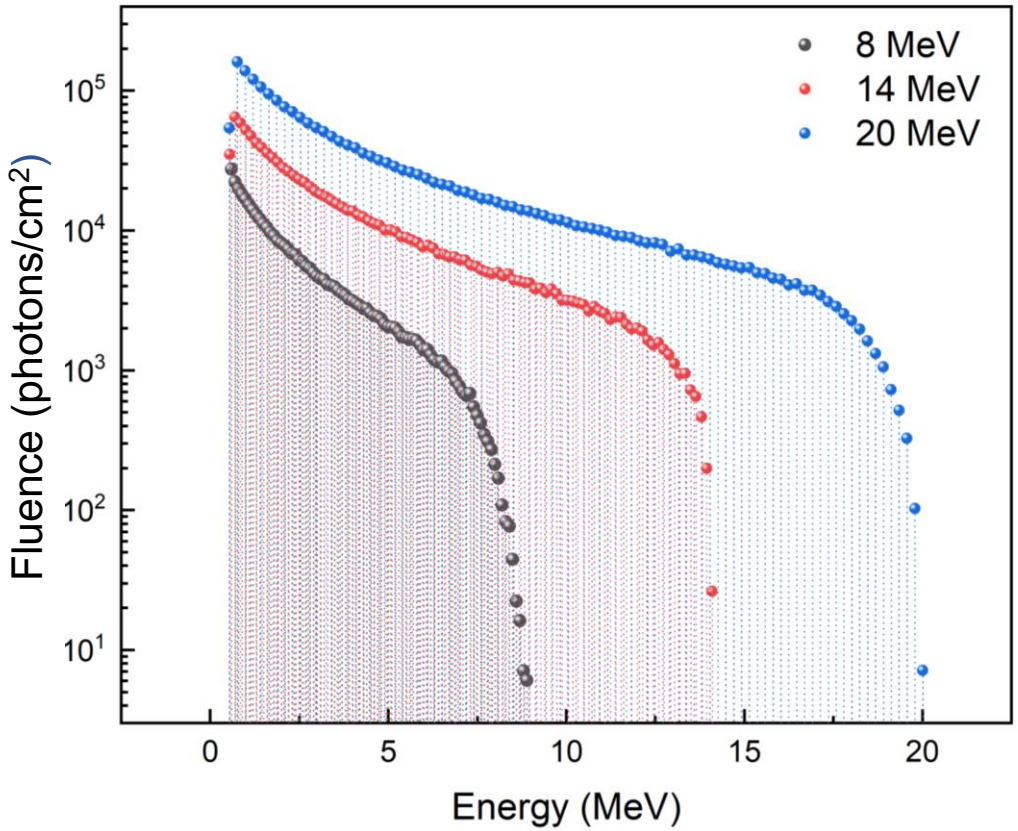

- MCNP6 model of linac end of irradiations to include linac geometry, radiator, beam scrub, current loop, target
- SDEF electron source using experimentally measured electron energy distribution and 200 point Akima spline fit
- Bremsstrahlung X-ray spectra needed in calculation of photofission events per pulse

Intensity Distribution of Beam on Target

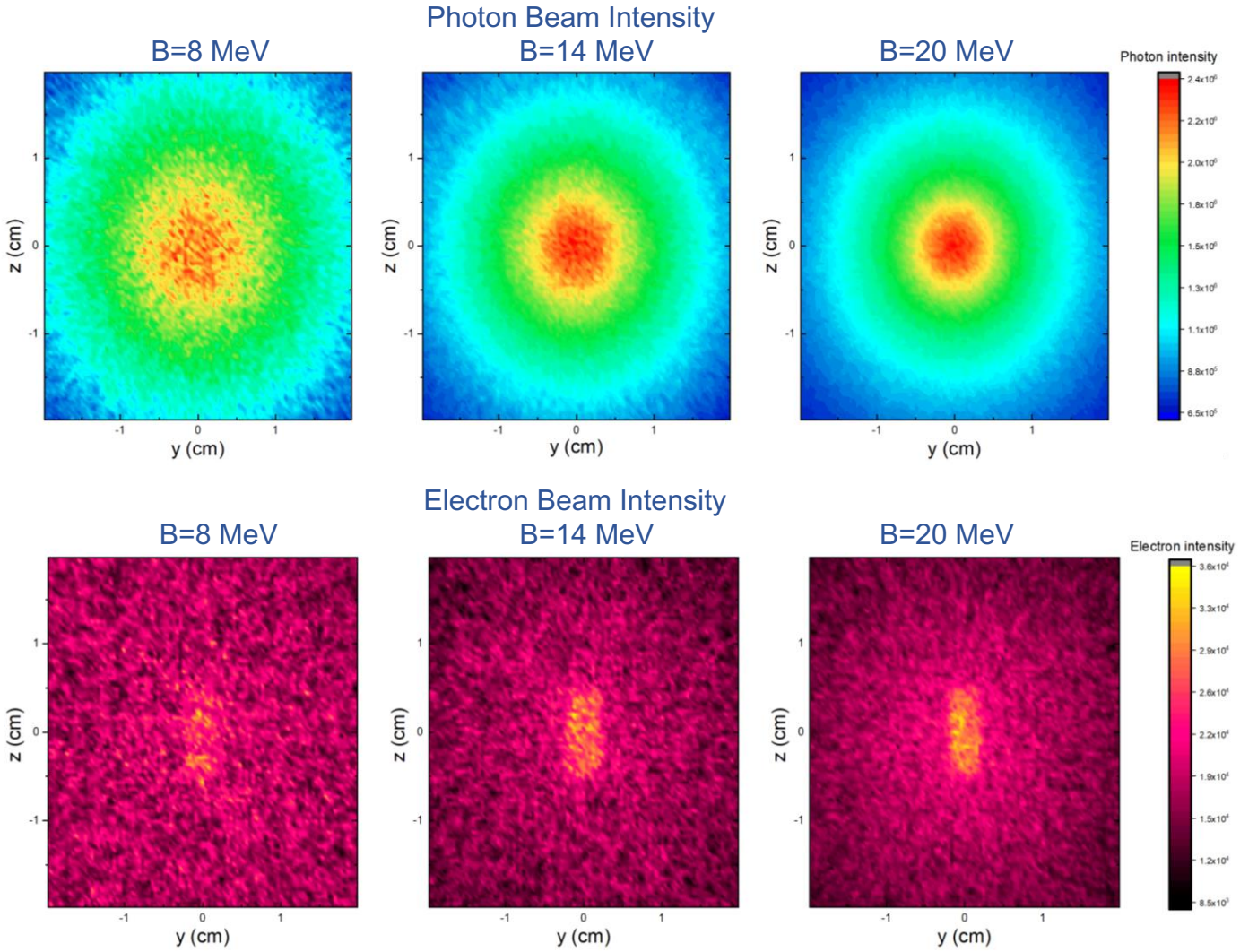

- Mesh tally of photon and electron distribution on target performed in MCNP6
- Visualize the spread of the beam and how photon beam is not uniform over target
- Electron tally shows placement of uranium foil from electron producing interactions
- Experimentally, “center” is determined from irradiation glass and aligning a laser

Uncertainty Contribution from Neutron Fission

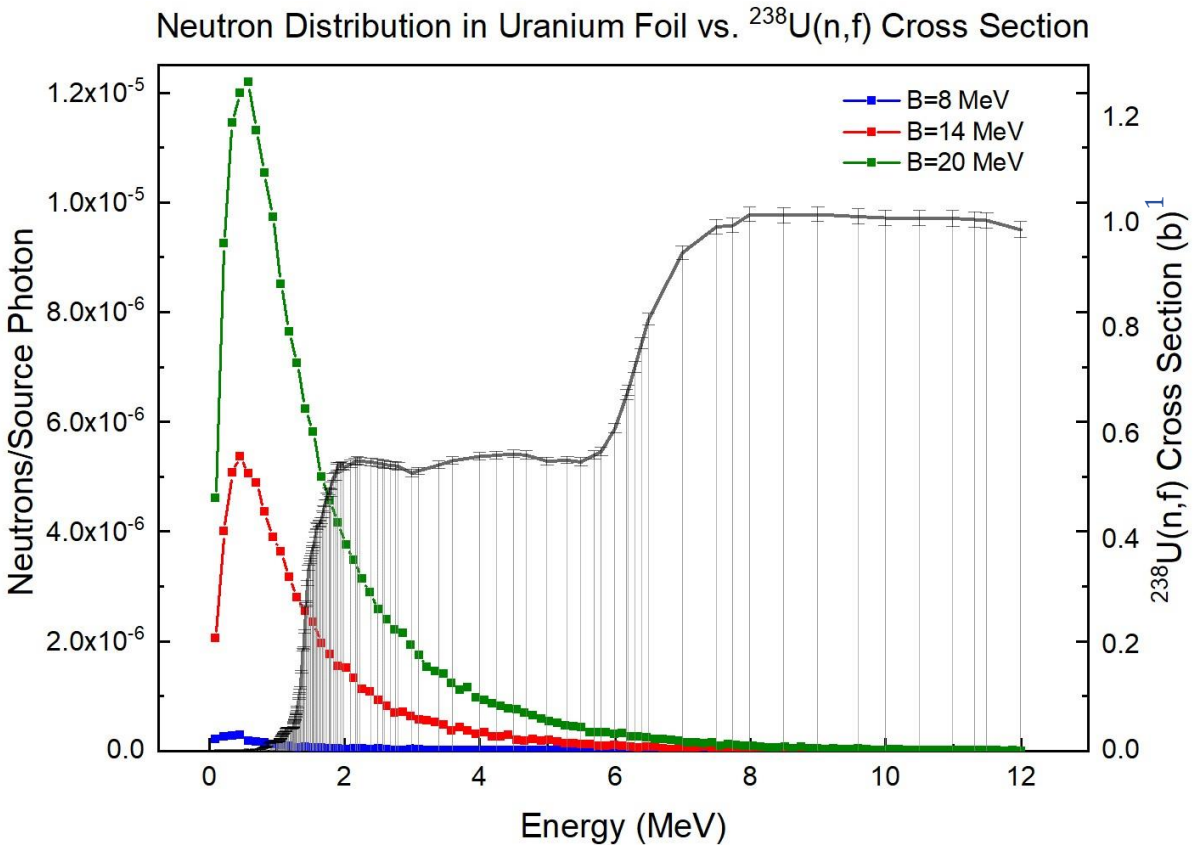

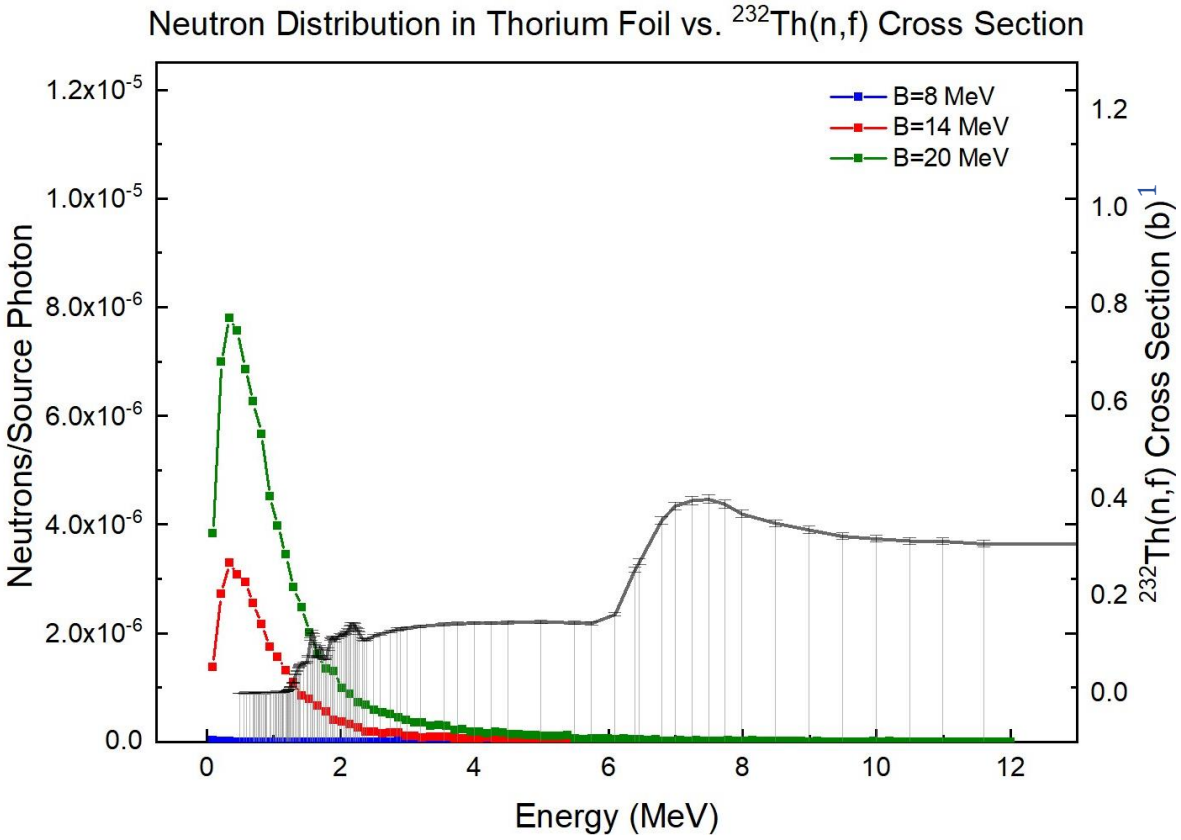

- Neutron flux on targets determined using MCNP6 simulation and ENDF-B/VII.0 neutron fission σ [1]
- Negligible contribution from neutron fission verified

[1] ENDF-B/VII.0: Accessed from Janis 4.0, Nuclear Energy Agency, Organization for Economic Co-operation and Development. https://www.oecd-nea.org/janis/

Uncertainty Contribution from Impurity Actinides

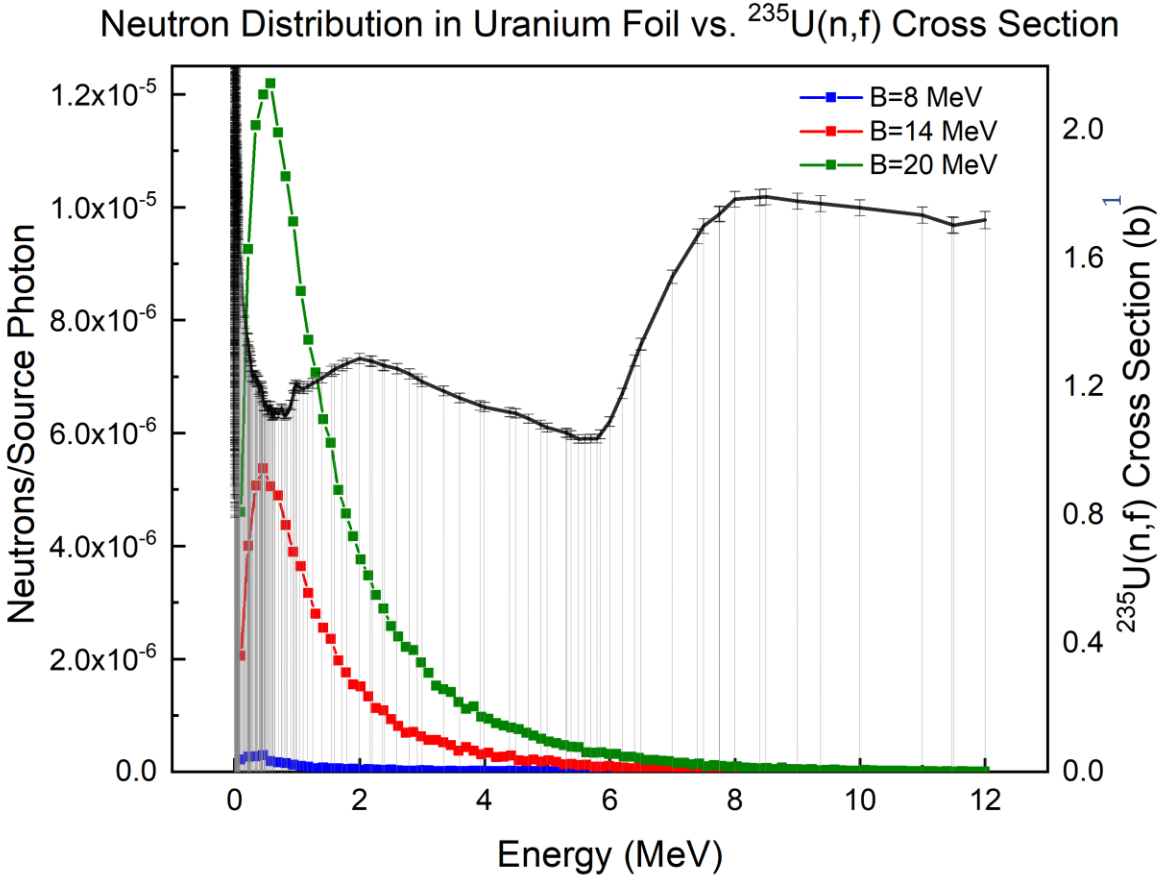

[1] ENDF-B/VII.0: Accessed from Janis 4.0, Nuclear Energy Agency, Organization for Economic Co-operation and Development. https://www.oecd-nea.org/janis/

- ICP-MS isotopic and elemental analysis performed on samples of the uranium and thorium foils at INL
- Uranium matches natural U standard with A=234 and 235
- Virtually no impurities of other thorium isotopes
- Photofission and neutron fission yield from ^{235}U impurity in uranium foil, negligible contribution

ICP-MS Isotopic Analysis of Uranium Foil

Sample	$^{234}\mathrm{U}(at.\%)$	$^{235}\mathrm{U}(at.\%)$	$^{238}\mathrm{U}(at.\%)$
U Foil	$0.0054\% \pm 0.0002\%$	$0.736\% \pm 0.009\%$	$99.26\% \pm 0.01\%$
Natural U Standard	$0.0055\% \pm 0.0002\%$	$0.720\% \pm 0.005\%$	$99.27\% \pm 0.01\%$

ICP-MS Isotopic Analysis of Thorium Foil

Sample	$^{228}\mathrm{Th}(at.\%)$	$^{229}\mathrm{Th}(at.\%)$	$^{230}\mathrm{Th}(at.\%)$	$^{232}\mathrm{Th}(at.\%)$
Th Foil	$< 1 \cdot 10^{-4}\%$	$< 1 \cdot 10^{-4}\%$	$< 1 \cdot 10^{-4}\%$	$99.99992\% \pm 0.00002\%$

Fission Product Yield Analysis

Pulsing and Cycling Structure

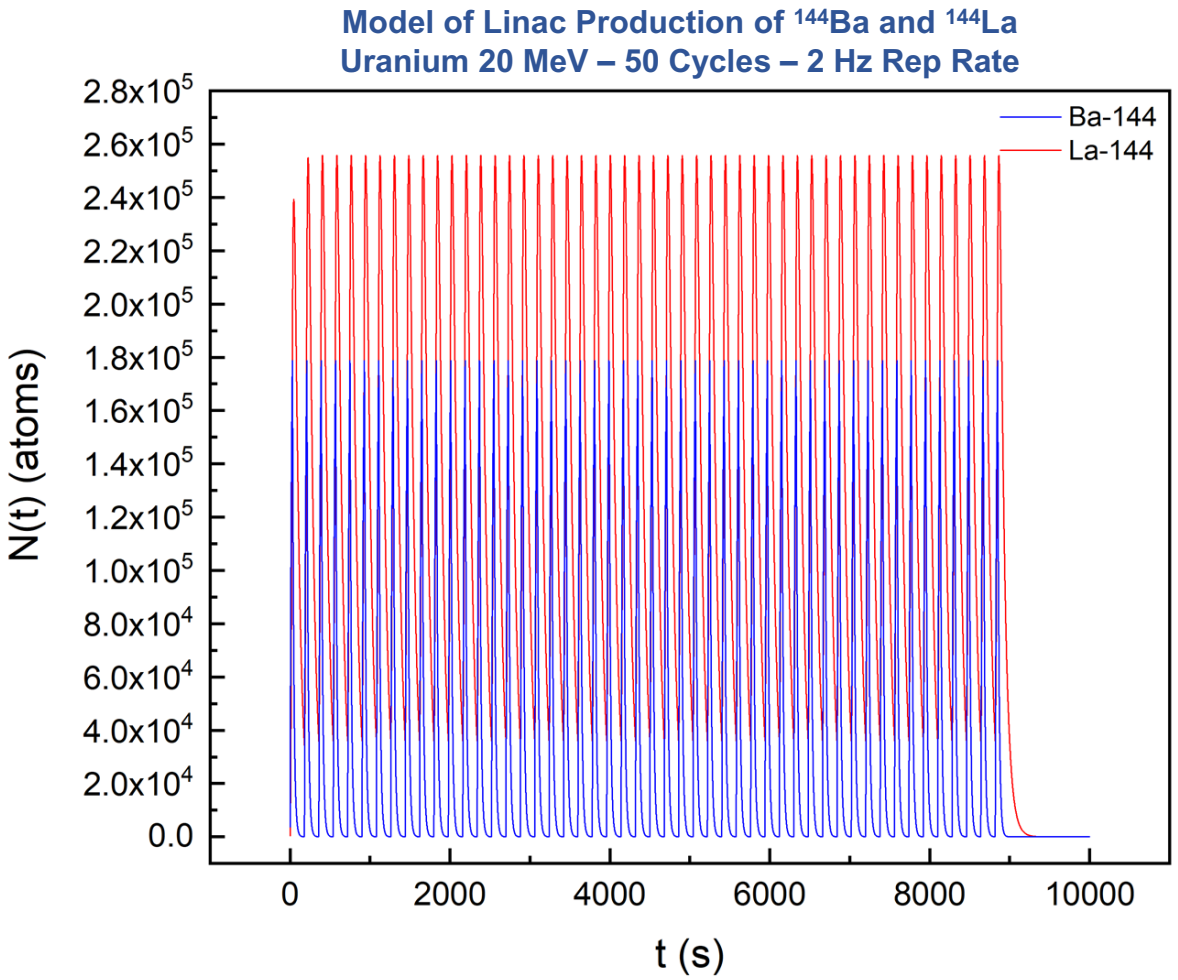

^{144}Ba ($T_{1/2}$=11.4 s) → ^{144}La ($T_{1/2}$=40.7 s)

- Pulsing of the accelerator leads to rapid buildup and decay during 30 second irradiation followed by measurement period
- To increase statistics, cycles of irradiation and measurement performed
- Measurements from in between each accelerator pulse summed
- Back-out per pulse contribution considering pulse and cycles

$$N(0)_{pp} = \frac{\frac{C}{\beta \varepsilon A_p} \cdot \frac{RT}{LT}}{\sum_{M=0}^{cycles-1} \sum_{m=0}^{pulses-1} \int_{t_1}^{t_2} \sum_{i}^{M} e^{(-\lambda(T_M - T_i) + t + (m\tau)} \lambda \, dt}$$

Temporal gamma ray spectroscopy

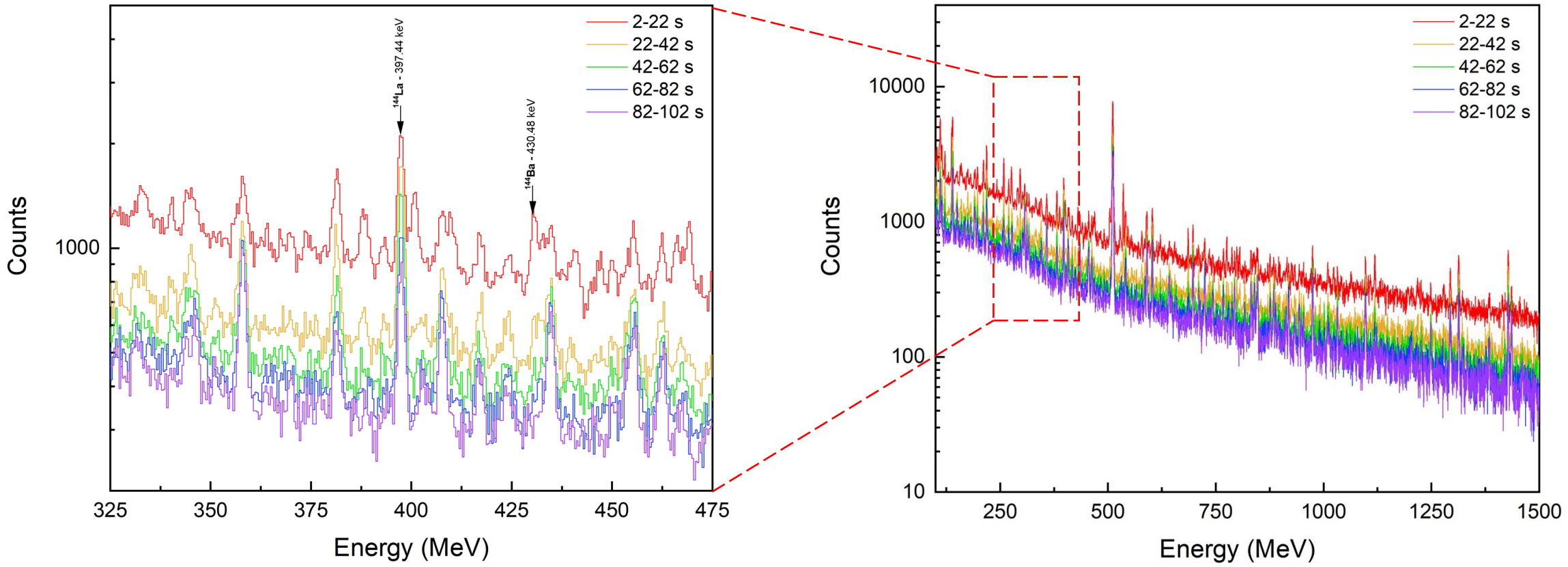

^{144}Ba ($T_{1/2}$=11.4 s) → ^{144}La ($T_{1/2}$=40.7 s)

$$R(t) = \frac{C}{\beta \varepsilon A_p}\frac{RT}{LT} = \int_{x-\frac{\Delta b}{2}}^{x+\frac{\Delta b}{2}} A(t)\, dE$$

Integral Decay Rate Fit

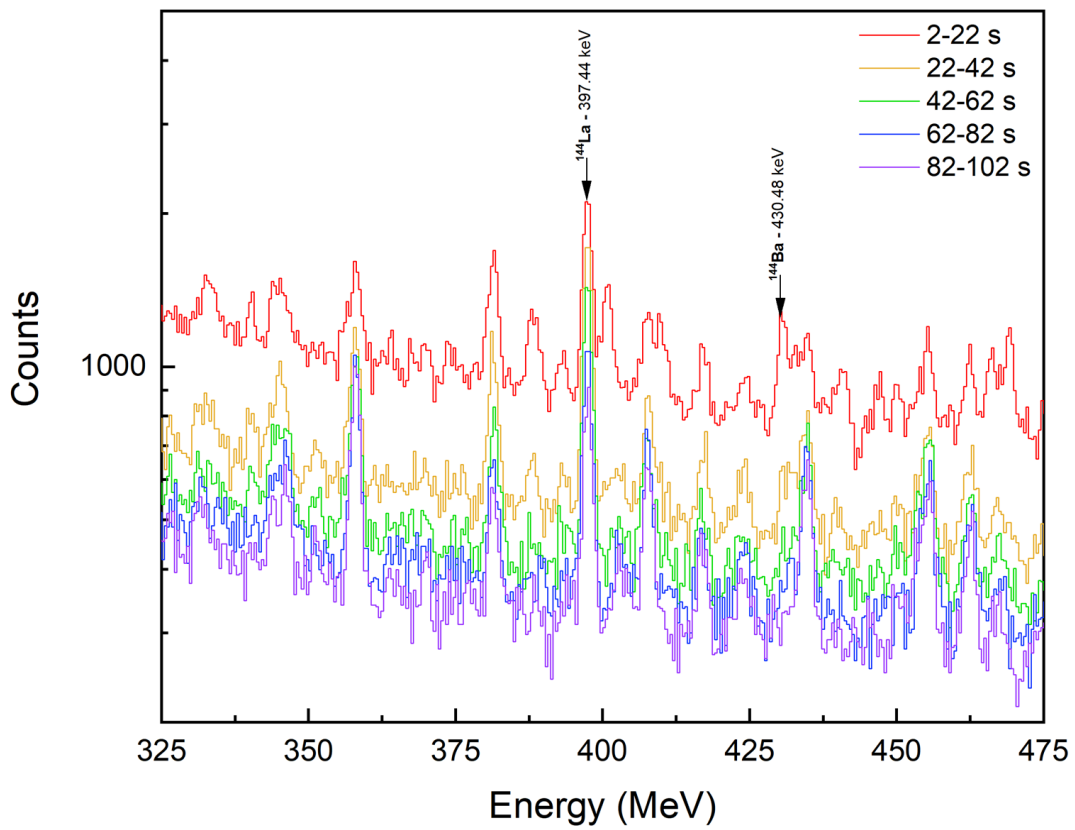

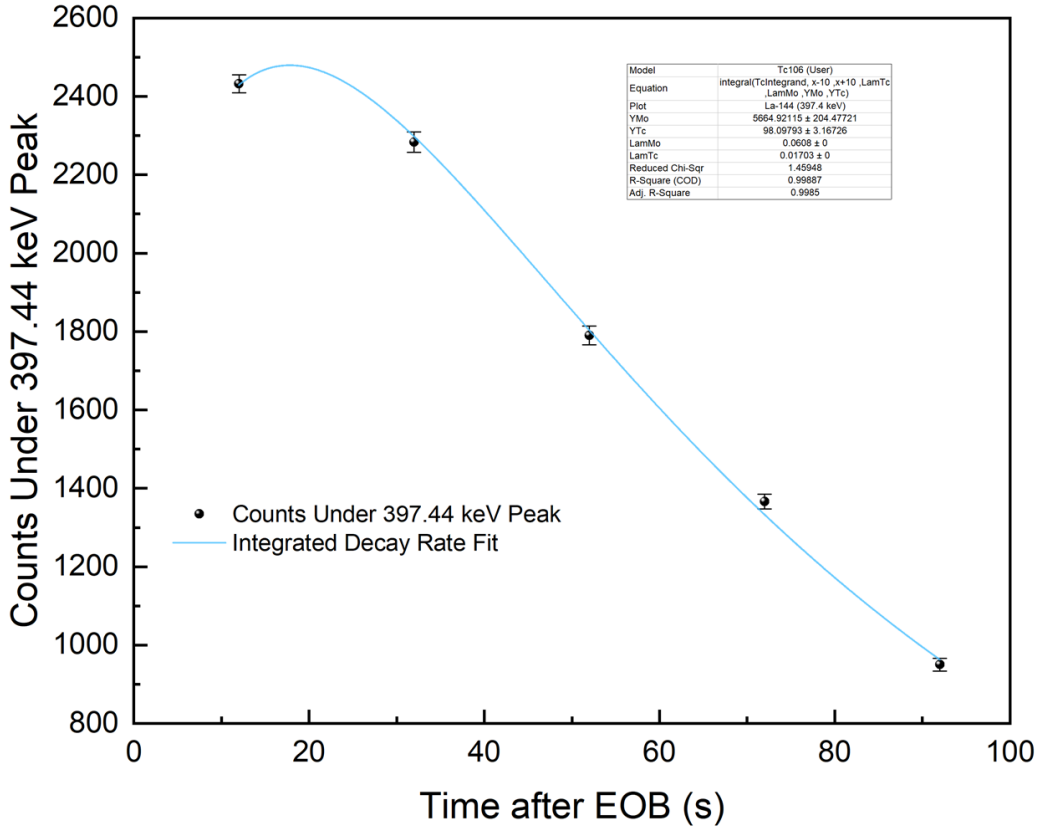

- Fit the individual bins with integrated activity to verify λ
- Also to solve for N_0 for all contributing nuclides

$$R(t) = \int_{x-10}^{x+10} \frac{\lambda_{La144}\lambda_{Ba144}}{\lambda_{La144} - \lambda_{Ba144}} N_{La144,0}\left[e^{-\lambda_{Ba144}x} - e^{-\lambda_{La144}x}\right] + \lambda_{Ba144} N_{Ba144,0} e^{-\lambda_{Ba144}x} dE$$

Photofissions per pulse from photonuclear cross sections

- Need photofission event yield per pulse for absolute FPY calculations
- For ^{238}U photofission yield per pulse, the ratio of σ(γ,f)/σ(γ,n) and ^{237}U production from 208.0 keV γ-ray peak
- For ^{232}Th photofission yield per pulse, the ratio of $\sigma_{U238}(\gamma,f)/\sigma_{Th232}(\gamma,f)$

Photofission Yield Per Linac Pulse

Target	B (MeV)	$\langle E^*(B)\rangle$ (MeV)	Fission Events Per Pulse
^{238}U	8	6.78±0.01	493±13
^{238}U	14	10.30±0.01	11,976±330
^{238}U	20	12.59±0.01	123,698±6,272
^{232}Th	8	6.74±0.02	374±10
^{232}Th	14	9.22±0.01	4951±156
^{232}Th	20	11.50±0.03	40,011±1552

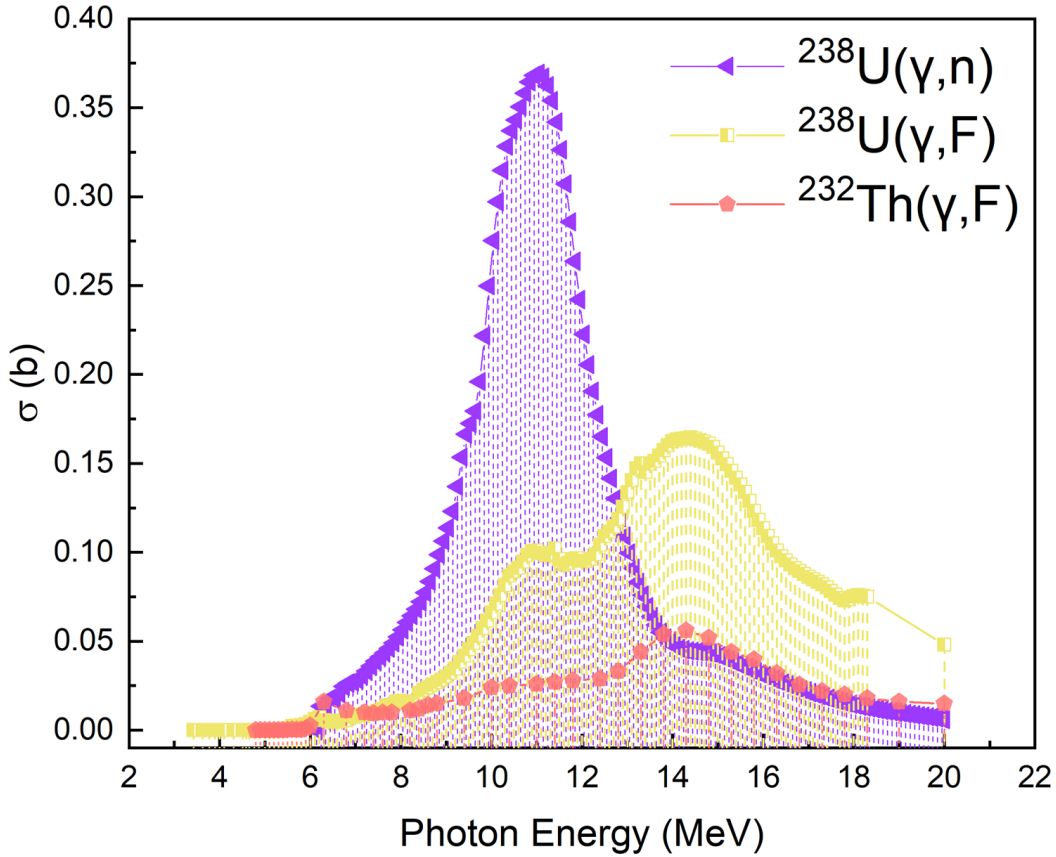

[1] ENDF-B/VII.0: Accessed from Janis 4.0, Nuclear Energy Agency, Organization for Economic Co-operation and Development. https://www.oecd-nea.org/janis/

Results

^{238}U Cumulative Fission Product Yields

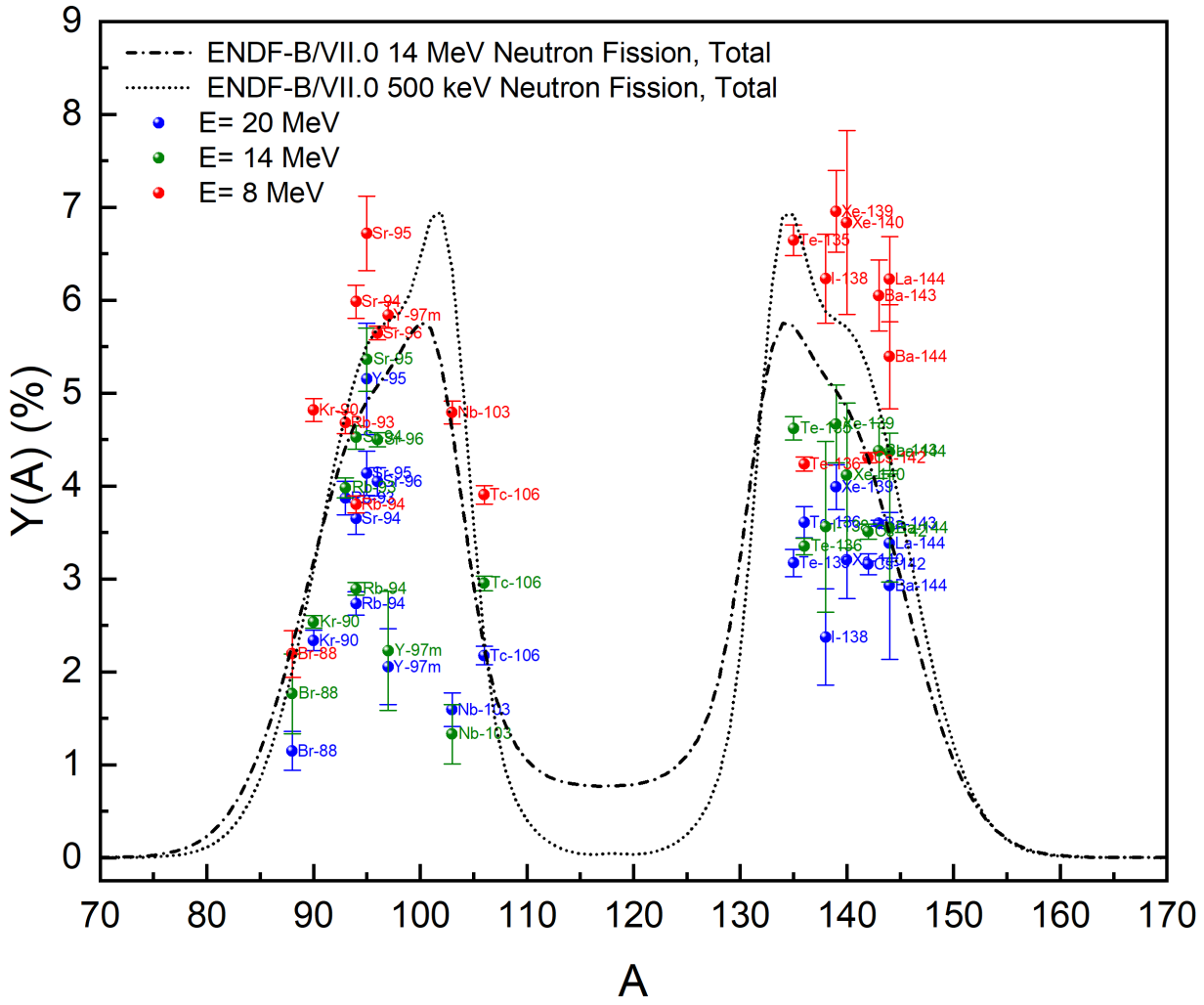

Cumulative Photofission Product Yields for ^{238}U								
A	Z	Nuclide	$T_{1/2}$ (s)	β	Energy (keV)	B=20 MeV	B=14 MeV	B=8 MeV
88	35	^{88}Br	16.34(8)	0.625(3)	775.28(6)	0.01149(21)	0.01762(43)	0.02193(25)
90	36	^{90}Kr	32.32(2)	0.390(3)	1118.69(5)	0.02337(11)	0.02536(7)	0.04817(12)
93	37	^{93}Rb	5.84(3)	0.202(1)	432.61(3)	0.03870(18)	0.03980(11)	0.04679(11)
94	37	^{94}Rb	2.702(5)	0.610(4)	836.9(1)	0.02736(13)	0.02893(7)	0.03802(9)
94	38	^{94}Sr	75.3(2)	0.942(9)	1427.7(1)	0.03652(17)	0.04522(12)	0.05983(18)
95	38	^{95}Sr	23.9(14)	0.226(12)	685.6(-)	0.04136(24)	0.05361(31)	0.06717(40)
96	38	^{96}Sr	1.07(1)	0.719(3)	809.4(3)	0.04045(15)	0.04499(8)	0.05647(73)
97	39	^{97m}Y	1.17(3)	0.921(2)	1103.3(3)	0.02054(41)	0.02226(64)	0.05840(14)
103	41	^{103}Nb	1.5(2)	1.00(6)	102.561(3)	0.01594(7)	0.01329(3)	0.04790(3)
106	43	^{106}Tc	35.6(6)	0.558(17)	270.096(9)	0.02175(10)	0.02951(8)	0.03904(10)
135	52	^{135}Te	19(2)	0.279(12)	603.70(3)	0.03172(15)	0.04621(13)	0.06645(17)
136	52	^{136}Te	17.63(9)	0.182(2)	578.75(3)	0.03610(17)	0.03350(9)	0.04236(7)
138	53	^{138}I	6.26(3)	0.56(3)	588.825(18)	0.02374(52)	0.03561(92)	0.06232(48)
139	54	^{139}Xe	39.68(14)	0.217(6)	296.53(7)	0.03989(24)	0.04667(42)	0.06956(44)
140	54	^{140}Xe	13.6(10)	0.20(2)	805.52(10)	0.03206(42)	0.04115(78)	0.06835(99)
142	55	^{142}Cs	1.684(14)	0.128(3)	1326.46(7)	0.03157(11)	0.03509(8)	0.04304(5)
143	56	^{143}Ba	14.5(3)	0.156(13)	798.79(2)	0.03599(30)	0.04390(30)	0.05550(123)
144	56	^{144}Ba	11.5(2)	0.183(4)	430.48(12)	0.02925(79)	0.03547(58)	0.04304(5)
144	57	^{144}La	40.8(4)	0.943(2)	397.44(9)	0.03384(16)	0.04368(20)	0.06226(36)

$$\langle E^*(B)\rangle = 12.59 \pm 0.01\ MeV$$
$$\langle E^*(B)\rangle = 10.30 \pm 0.01\ MeV$$
$$\langle E^*(B)\rangle = 6.78 \pm 0.01\ MeV$$

^{232}Th Cumulative Fission Product Yields

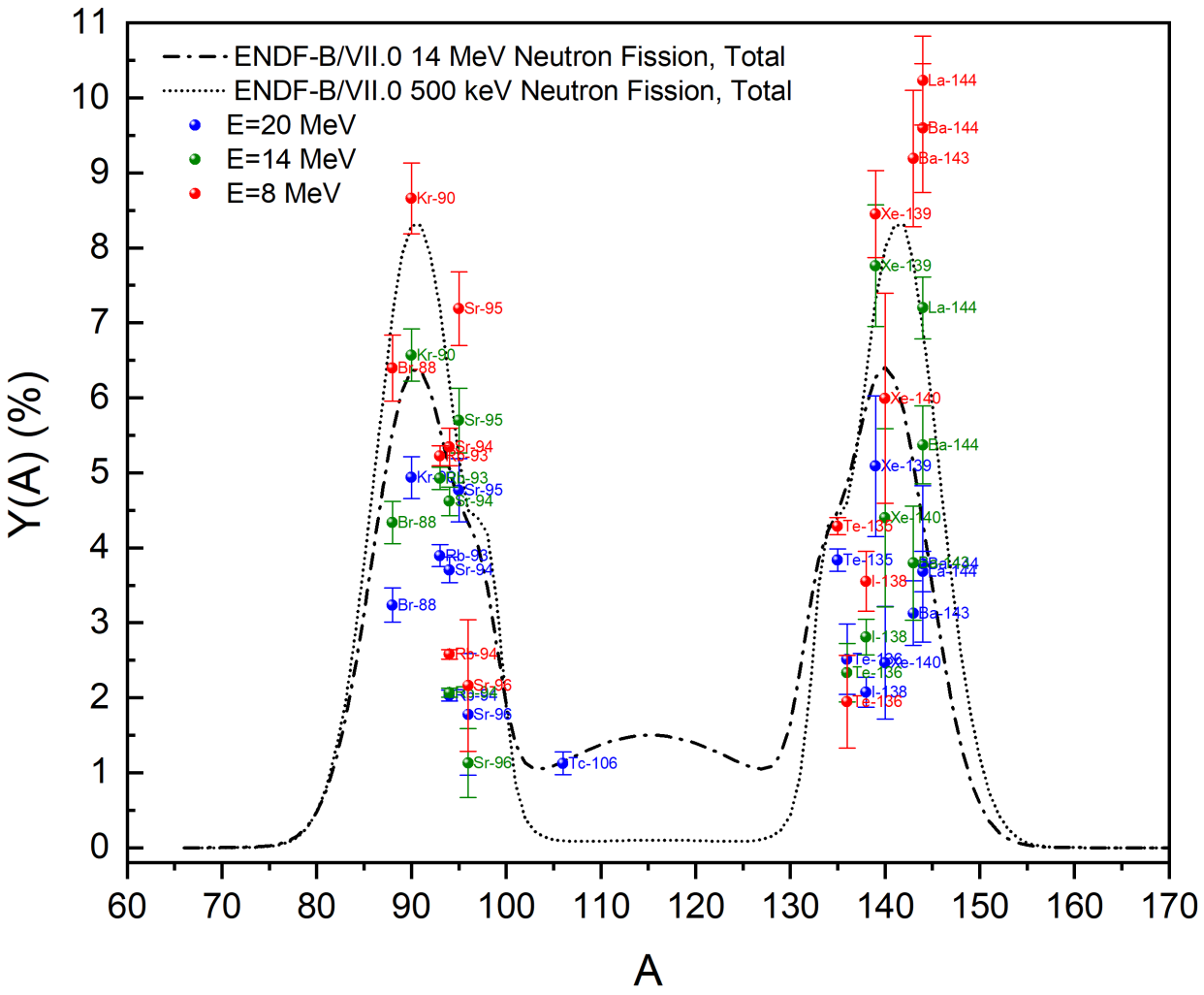

Cumulative Photofission Product Yields for ^{232}Th								
A	Z	Nuclide	$T_{1/2}$ (s)	β	Energy (keV)	B=20 MeV	B=14 MeV	B=8 MeV
88	35	^{88}Br	16.34(8)	0.625(3)	775.28(6)	0.03236(23)	0.04337(28)	0.06395(44)
90	36	^{90}Kr	32.32(2)	0.390(3)	1118.69(5)	0.04936(28)	0.06570(35)	0.08660(47)
93	37	^{93}Rb	5.84(3)	0.202(1)	432.61(3)	0.03894(15)	0.04925(15)	0.05225(13)
94	37	^{94}Rb	2.702(5)	0.610(4)	836.9(1)	0.02028(7)	0.02067(6)	0.02579(9)
94	38	^{94}Sr	75.3(2)	0.942(9)	1427.7(1)	0.03705(17)	0.04622(19)	0.05344(25)
95	38	^{95}Sr	23.9(14)	0.226(12)	685.6(-)	0.04683(42)	0.05698(43)	0.07190(49)
96	38	^{96}Sr	1.07(1)	0.719(3)	809.4(3)	0.01778(81)	0.01128(46)	0.02163(73)
106	43	^{106}Tc	35.6(6)	0.558(17)	270.096(9)	0.01126(15)	-	-
135	52	^{135}Te	19(2)	0.279(12)	603.70(3)	0.03836(15)	-	0.04288(11)
136	52	^{136}Te	17.63(9)	0.182(2)	578.75(3)	0.02513(75)	0.02332(39)	0.01948(62)
138	53	^{138}I	6.26(3)	0.56(3)	588.825(18)	0.02074(20)	0.02810(24)	0.03552(40)
139	54	^{139}Xe	39.68(14)	0.217(6)	296.53(7)	0.05088(94)	0.07762(81)	0.08452(58)
140	54	^{140}Xe	13.6(10)	0.20(2)	805.52(10)	0.02467(75)	0.04399(119)	0.05993(140)
143	56	^{143}Ba	14.5(3)	0.156(13)	798.79(2)	0.03054(43)	0.03704(76)	0.08972(91)
144	56	^{144}Ba	11.5(2)	0.183(4)	430.48(12)	0.03785(104)	0.05370(52)	0.09596(86)
144	57	^{144}La	40.8(4)	0.943(2)	397.44(9)	0.03682(27)	0.07199(41)	0.10232(59)

$$\langle E^*(B) \rangle = 11.50 \pm 0.03\ MeV$$

$$\langle E^*(B) \rangle = 9.22 \pm 0.01\ MeV$$

$$\langle E^*(B) \rangle = 6.74 \pm 0.02\ MeV$$

Distribution of ^{238}U and ^{232}Th FPY

Uranium-238

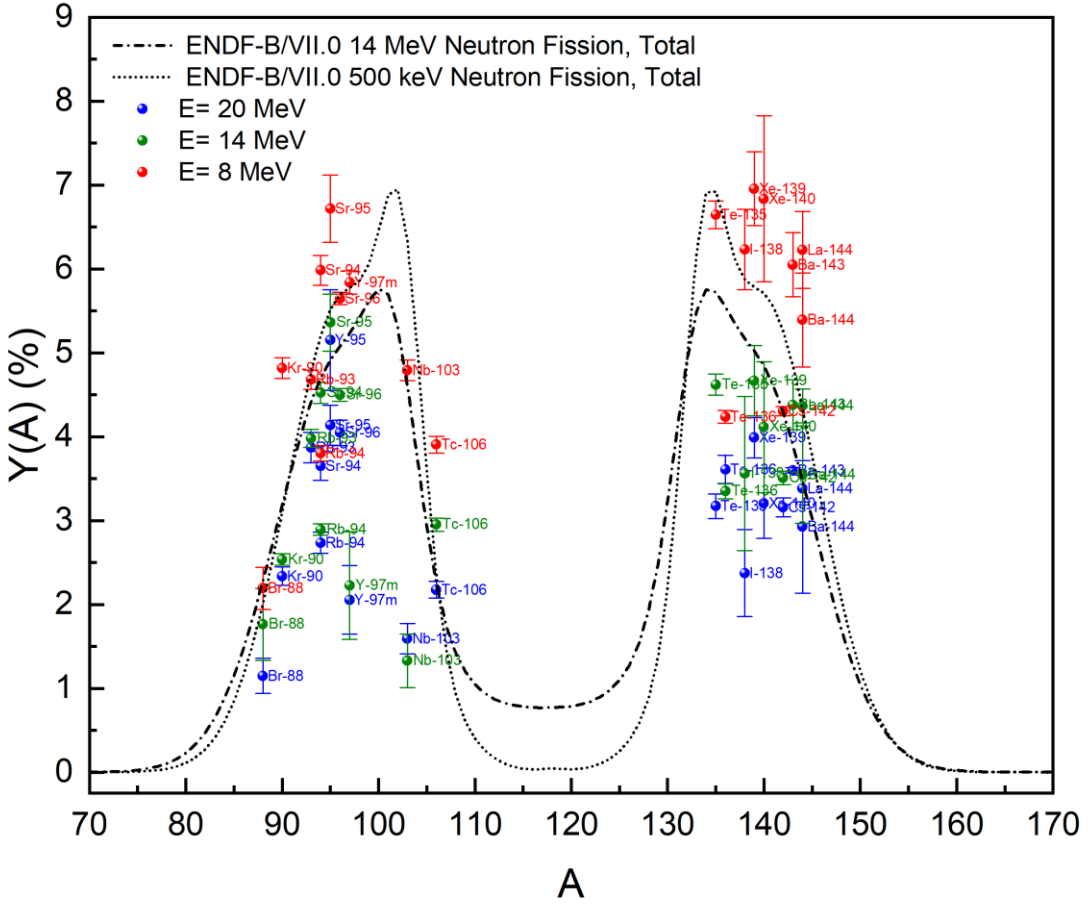

Thorium-232

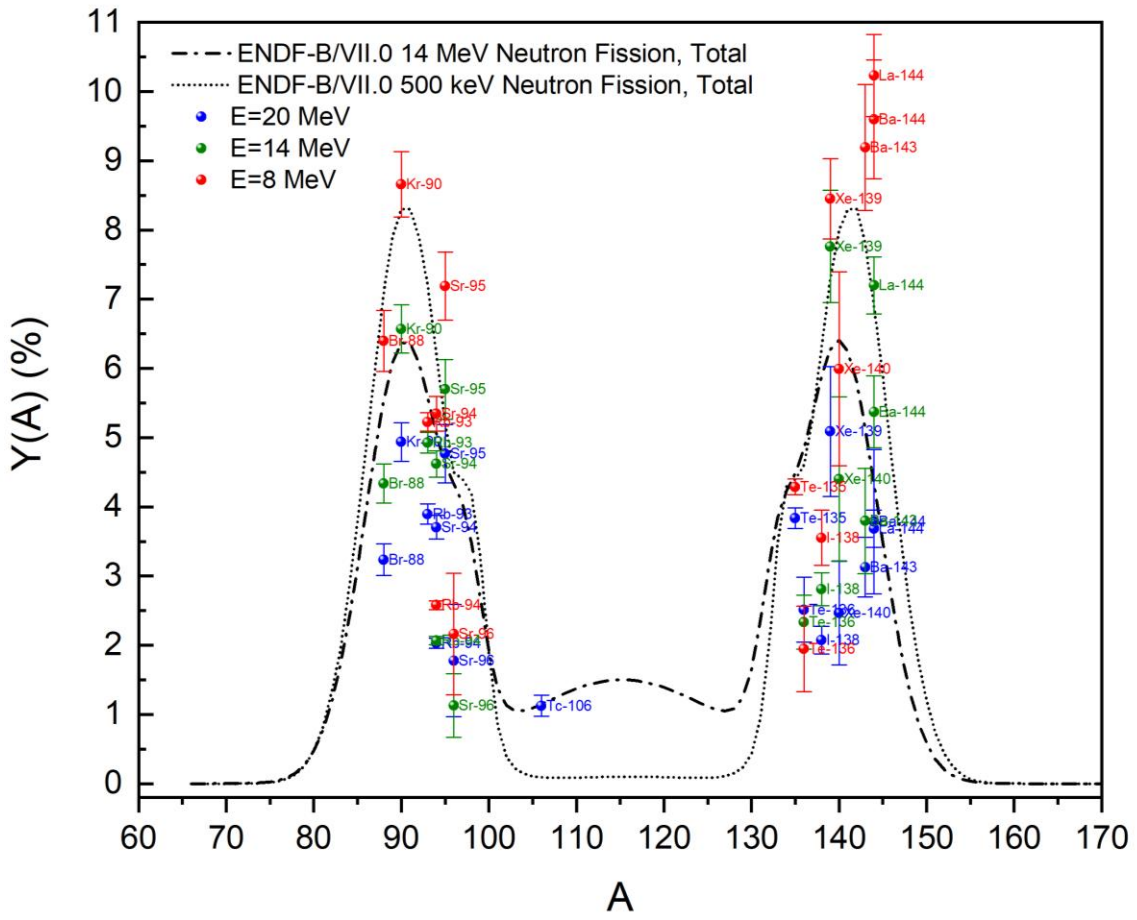

Conclusion

Conclusions

- Short-lived products reported for ^{238}U and ^{232}Th for 3 endpoint energies, reported with both endpoint and excitation energies to allow for comparison
  - CFPYs for 20 MeV good agreement with DT neutron fission
  - CFPYs for 14 and 8 MeV reflect expected distribution using the ENDF-B/VII.0 fractional mass yields and multimode -fission model
- Absolute uncertainty reported with all factors considered where data was available or acquired through simulation
- Photofission product yields measured for lower (≤12 MeV) excitation energy to be most useful for forensics applications

Questions?

Supplemental Slides

HPGe Detector and Instrumentation

In-Hall Instrumentation

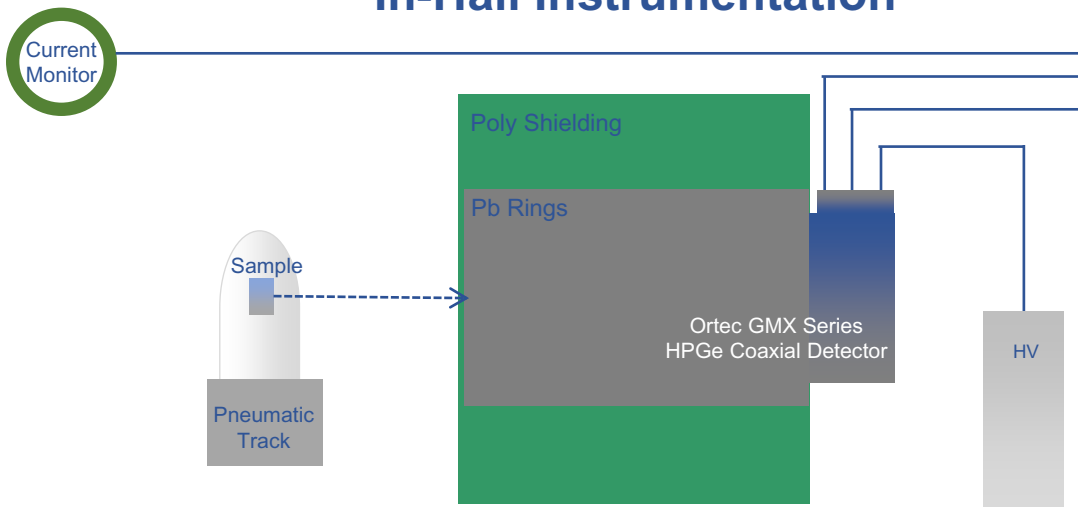

- Ortec GMX Series HPGe Coaxial detector
  - N-type 40% efficiency
  - Mechanically-cooled
- High Voltage Bias = -2,000 V
- Preamplifier 2 outputs sent via BNC to control room
- Pearson current monitor on output of linac

Control Room Instrumentation

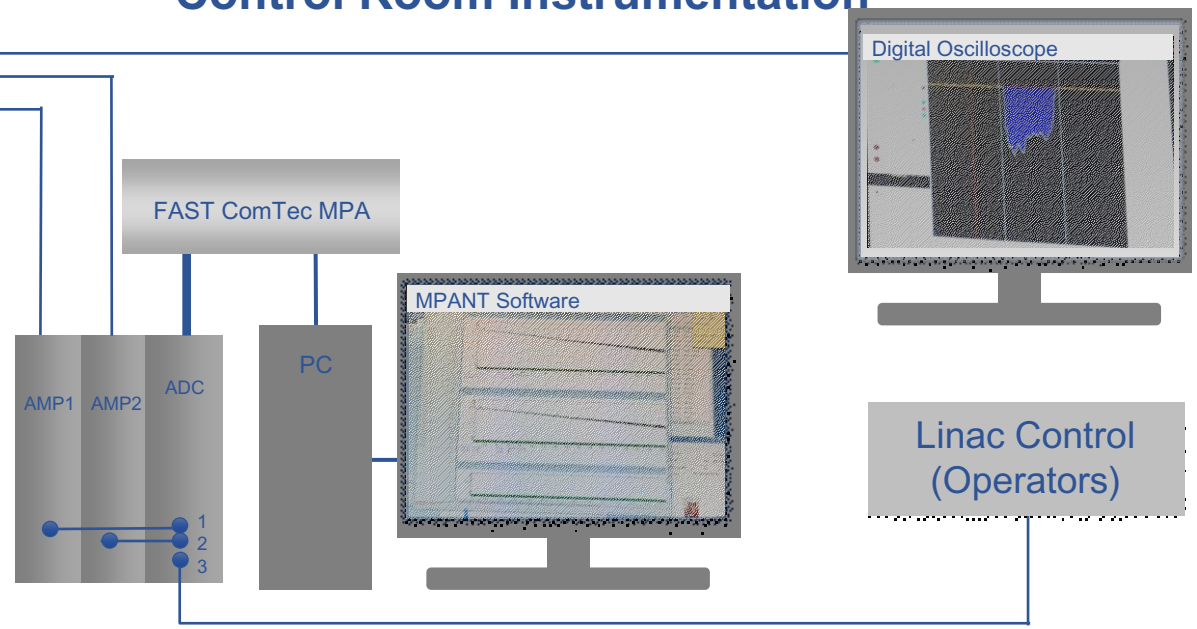

- 2 amplifiers to shape preamplifier signal
  - ADC1 Range: 50 keV to 3.5 MeV
  - ADC2 Range: 50 keV to 2 MeV
- Analog-to-digital converter
- FAST ComTec MPA
  - Produces list-mode data
- PC to verify real-time measurements

Bremsstrahlung X-Ray Production

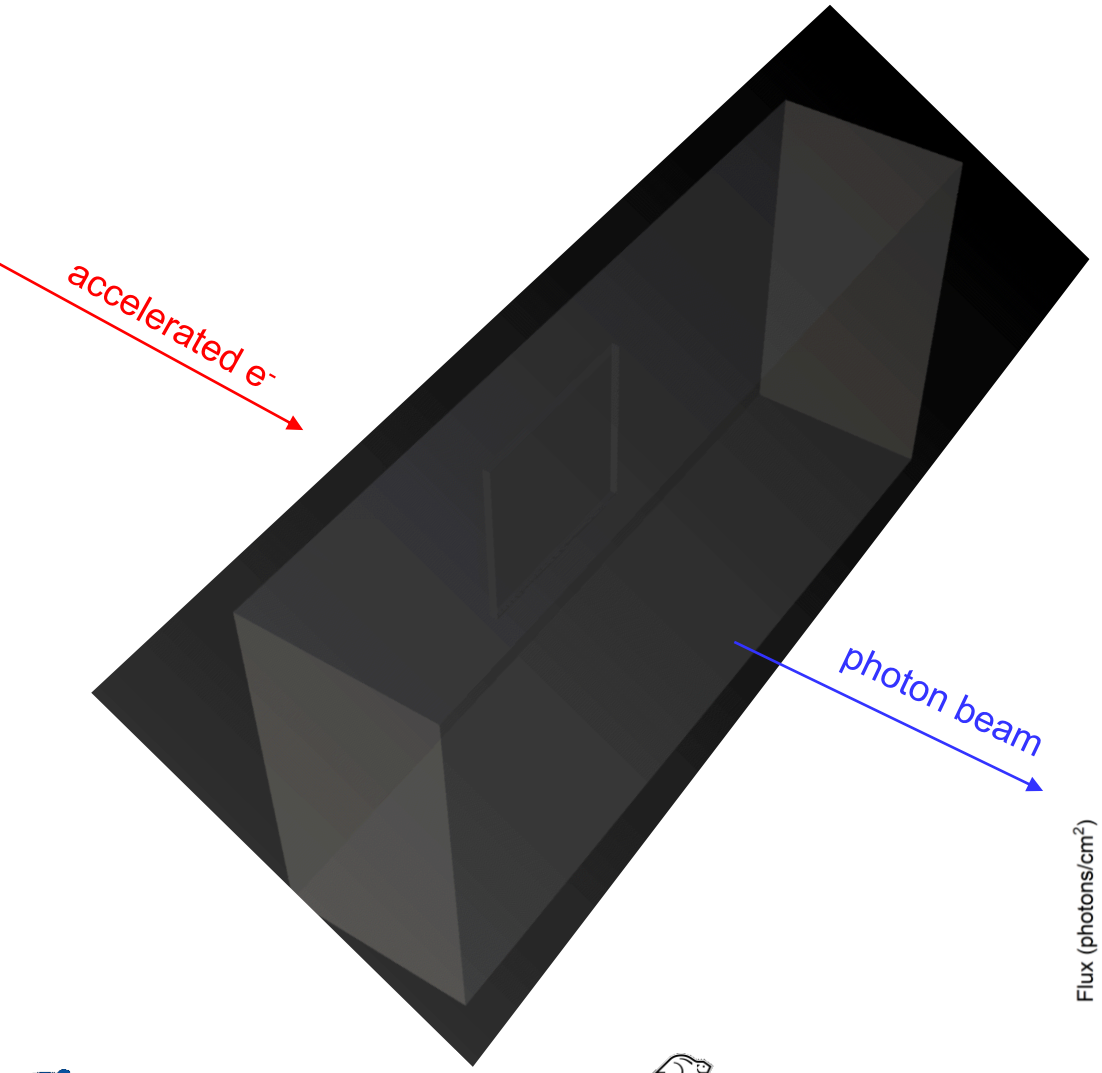

- Linac produces high energy electron beam
  - Operators control energy of these accelerated e^-
- 0.22 cm thick W radiator/converter to convert electron beam to bremsstrahlung photon spectra
- W Converter is embedded in aluminum beam scrub, requires intense cooling
- Bremsstrahlung X-ray spectra produced from deceleration of e^- beam

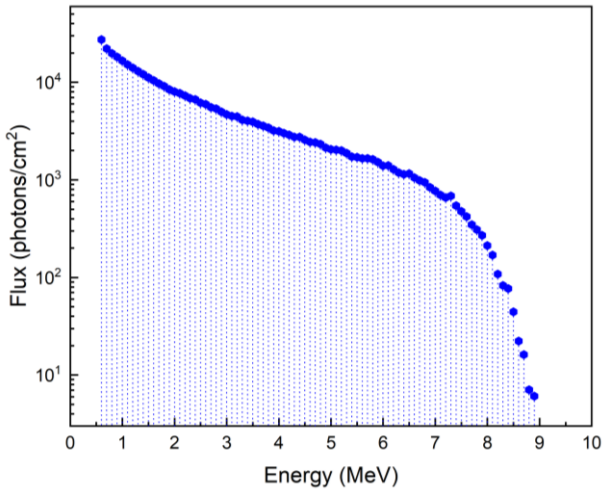

- Resulting energy spectrum depends on target and incident electron energy
- Maximum energy of bremsstrahlung spectra (endpoint energy) equal to the maximum electron energy

Integral Decay Rate Fit

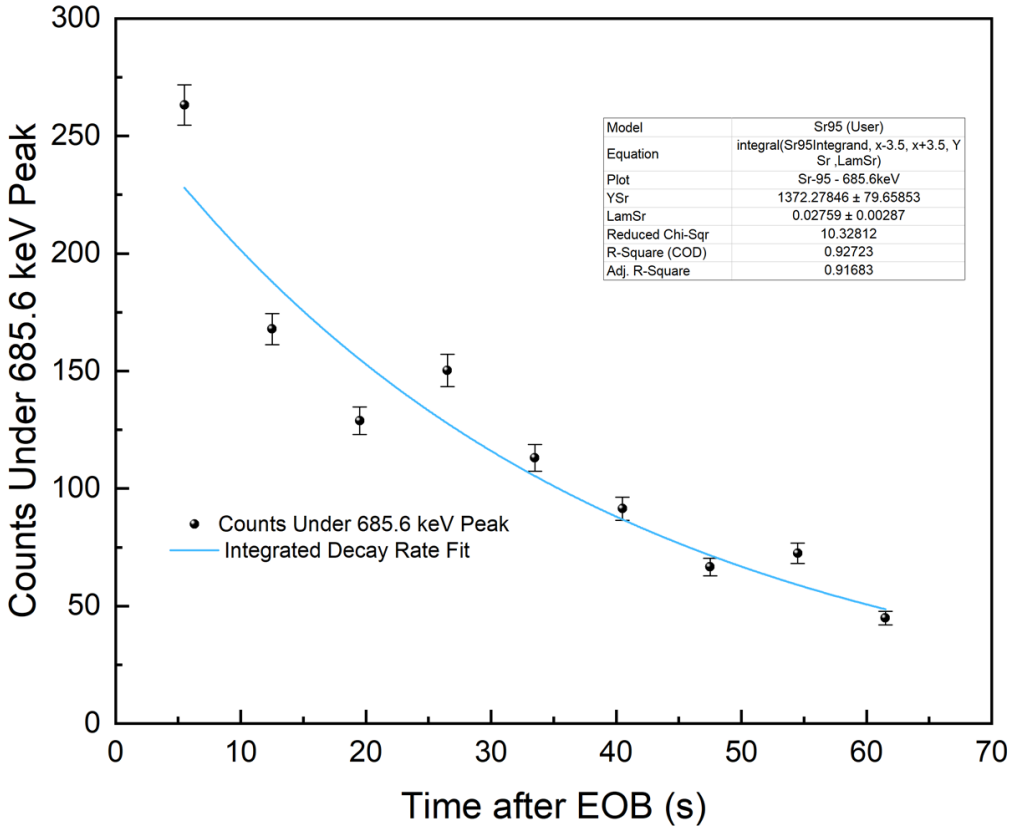

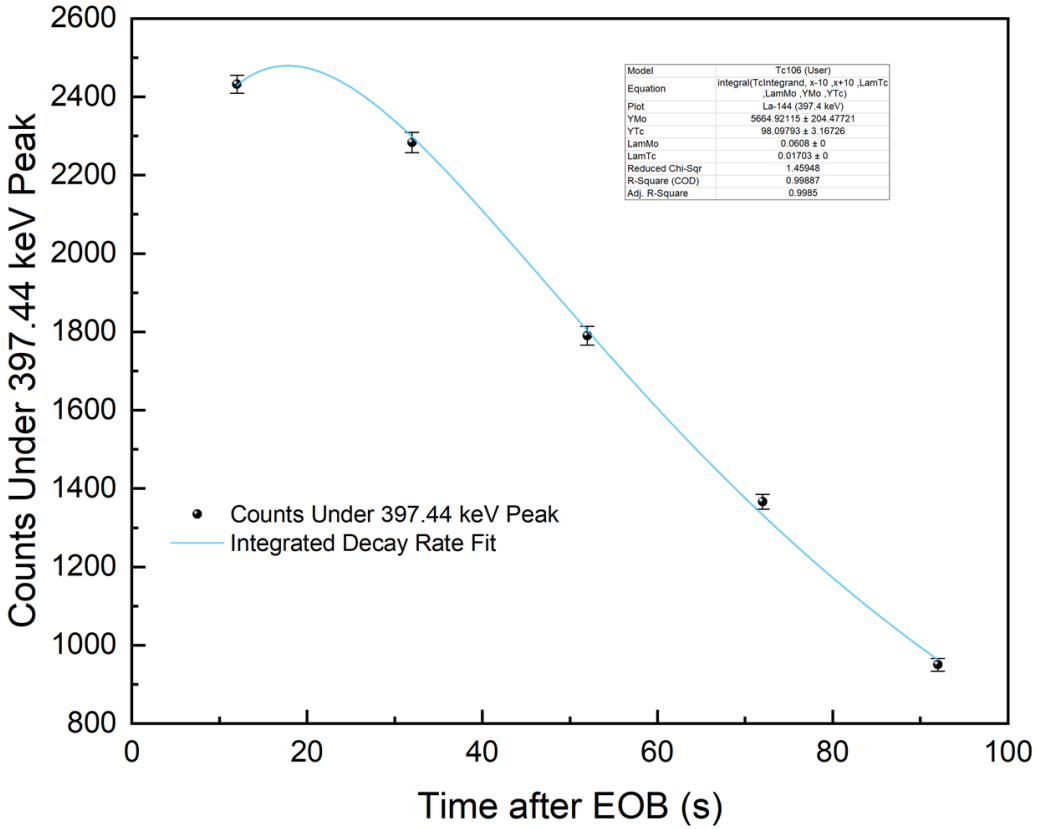

$$R(t) = \int_{x-2.5}^{x+2.5} \lambda_{Sr95} N_{Sr95,0} e^{-\lambda_{Sr95} x} dE$$

- If parent decays fully prior to counts, not contributing to peak and not included

^{95}Kr ($T_{1/2}$=114 ms) → ^{95}Rb ($T_{1/2}$=377 ms) → ^{95}Sr ($T_{1/2}$=25.1s)

Optimization of parsing

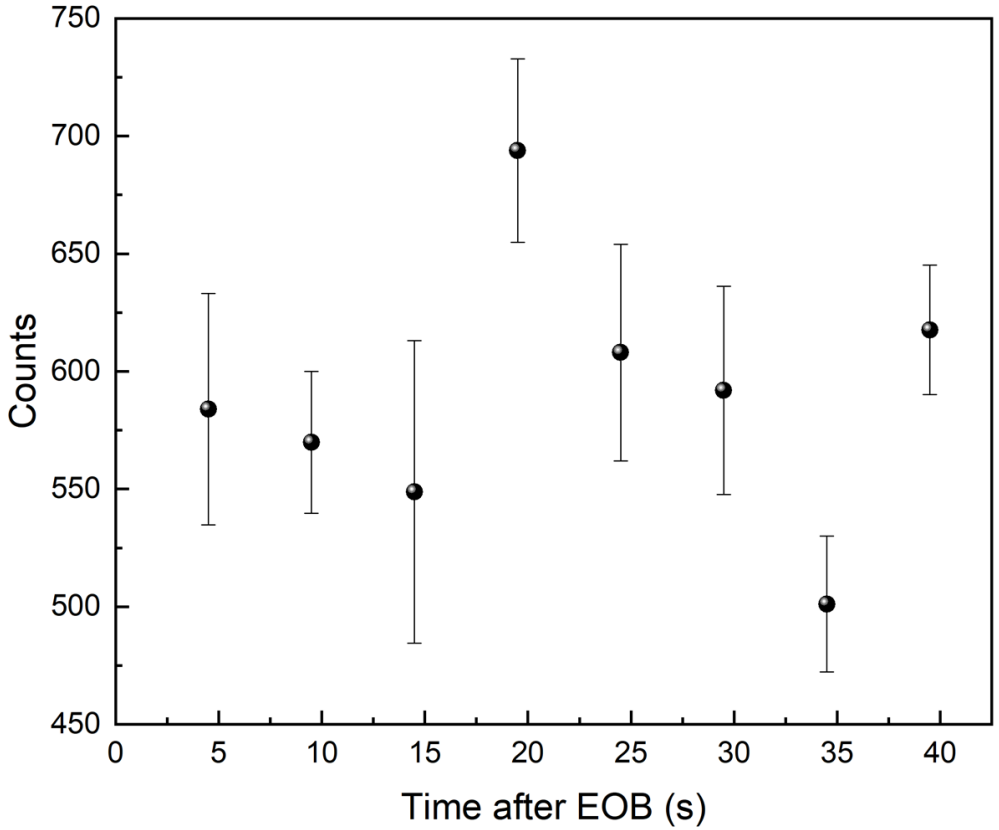

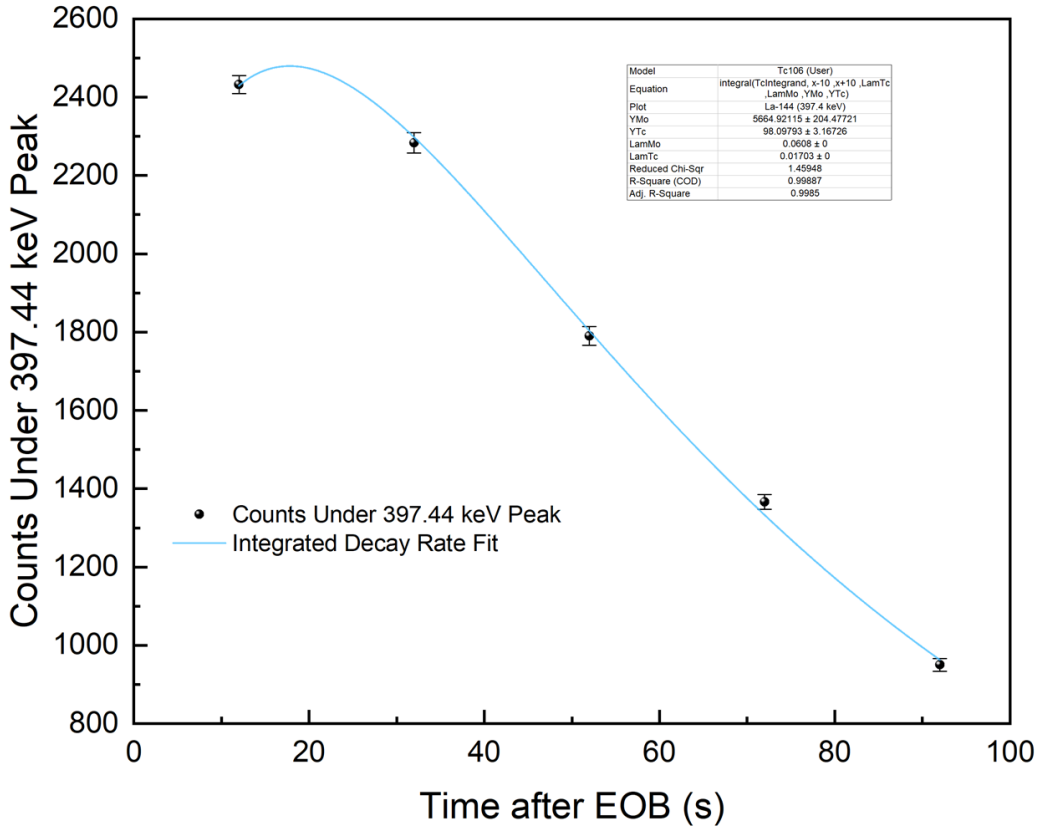

- Parsed to timing bins about ½ the half-life of nuclide of interest to optimize statistics
- Some parsing resulted in sufficient statistics to fit for solving

HPGe Detector Efficiency

- Model of absolute efficiency for the in-hall HPGe detection setup to include uncertainty at any energy: ADC1 and ADC2

- Includes uncertainty contribution from:
  - Nuclear data accessed from ENSDF[2] ($T_{1/2}$ and β)
  - Activity reported for each calibrated check source from the manufacturer
  - Counts measured under γ-ray peak

- Use of partial error and micro-correlation matrix to include dependence from γ-ray energies originating from the same nuclide

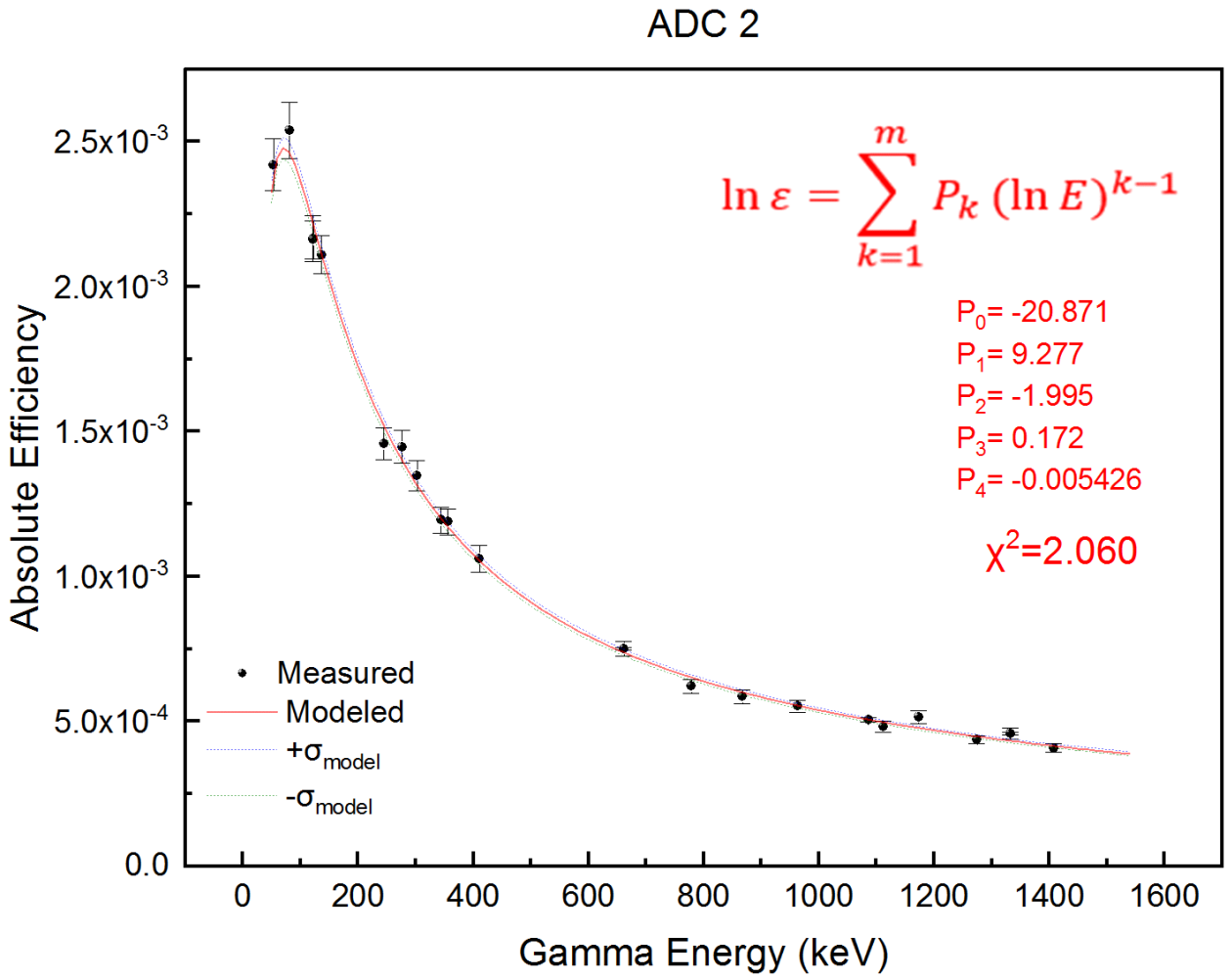

[2] ENSDF: Evaluated Nuclear Structure Data File Search and Retrieval, National Nuclear Data Center. https://www.nndc.bnl.gov/ensdf/
L. Geraldo and D. Smith, "Covariance analysis and fitting of germanium gamma-ray detector efficiency calibration data," NIM A: vol. 290, no. 2, pp. 499-508, 1990.

Model of HPGe Response

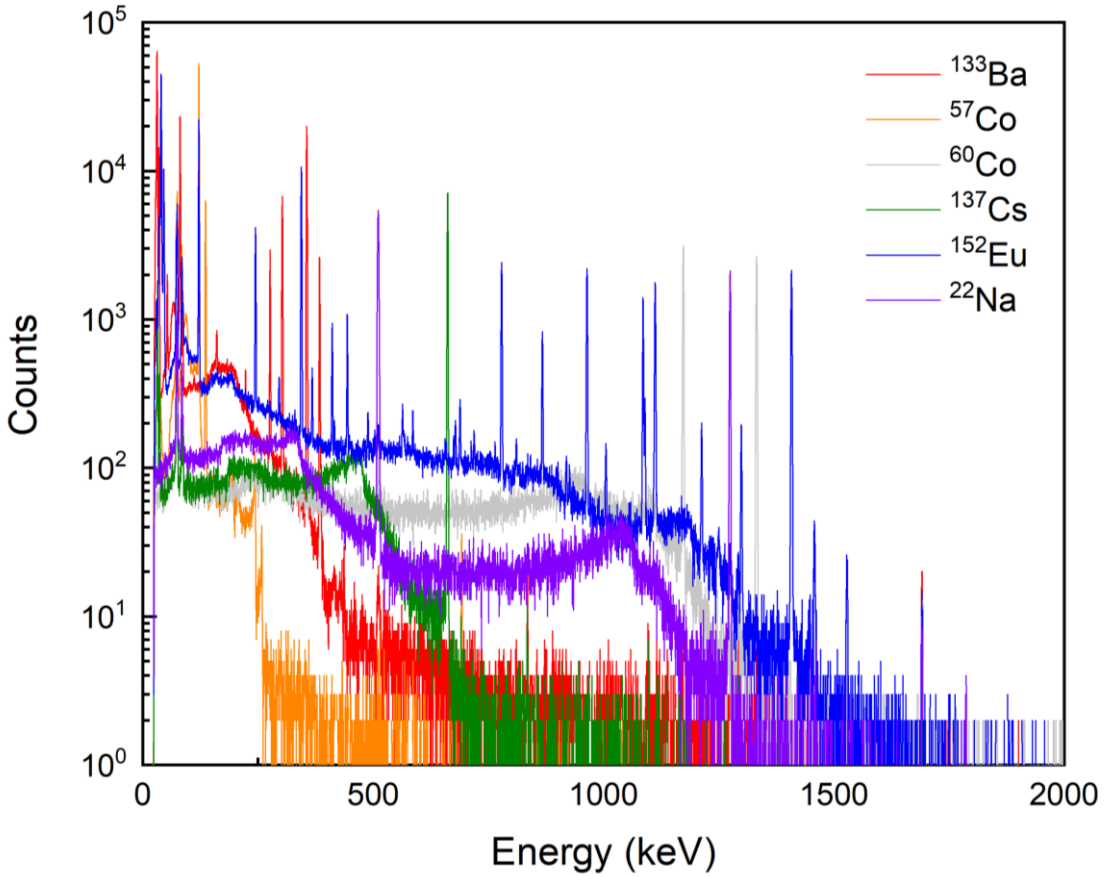

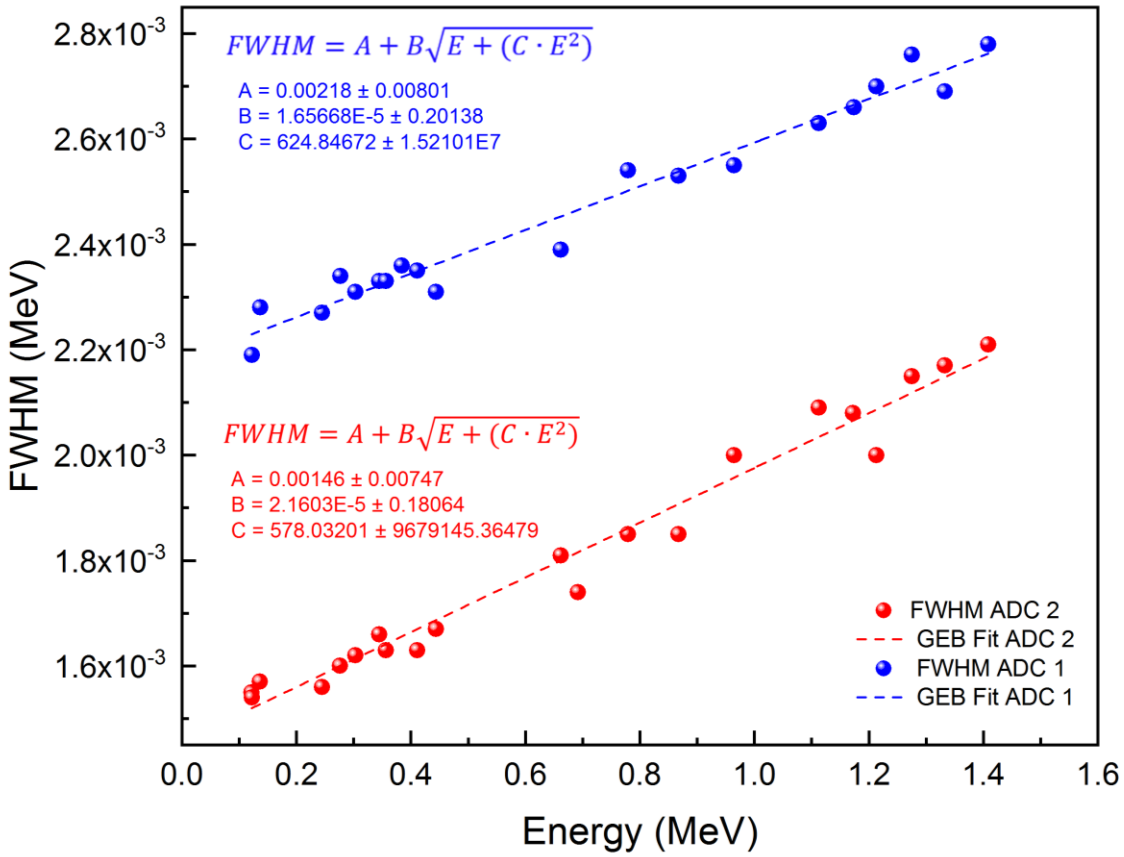

- High-fidelity model of high-purity germanium (HPGe) spectroscopic response using MCNP6
- Resolution of check source γ-rays measured from energy calibration measurements and fit to determine FWHM

Model of HPGe Response

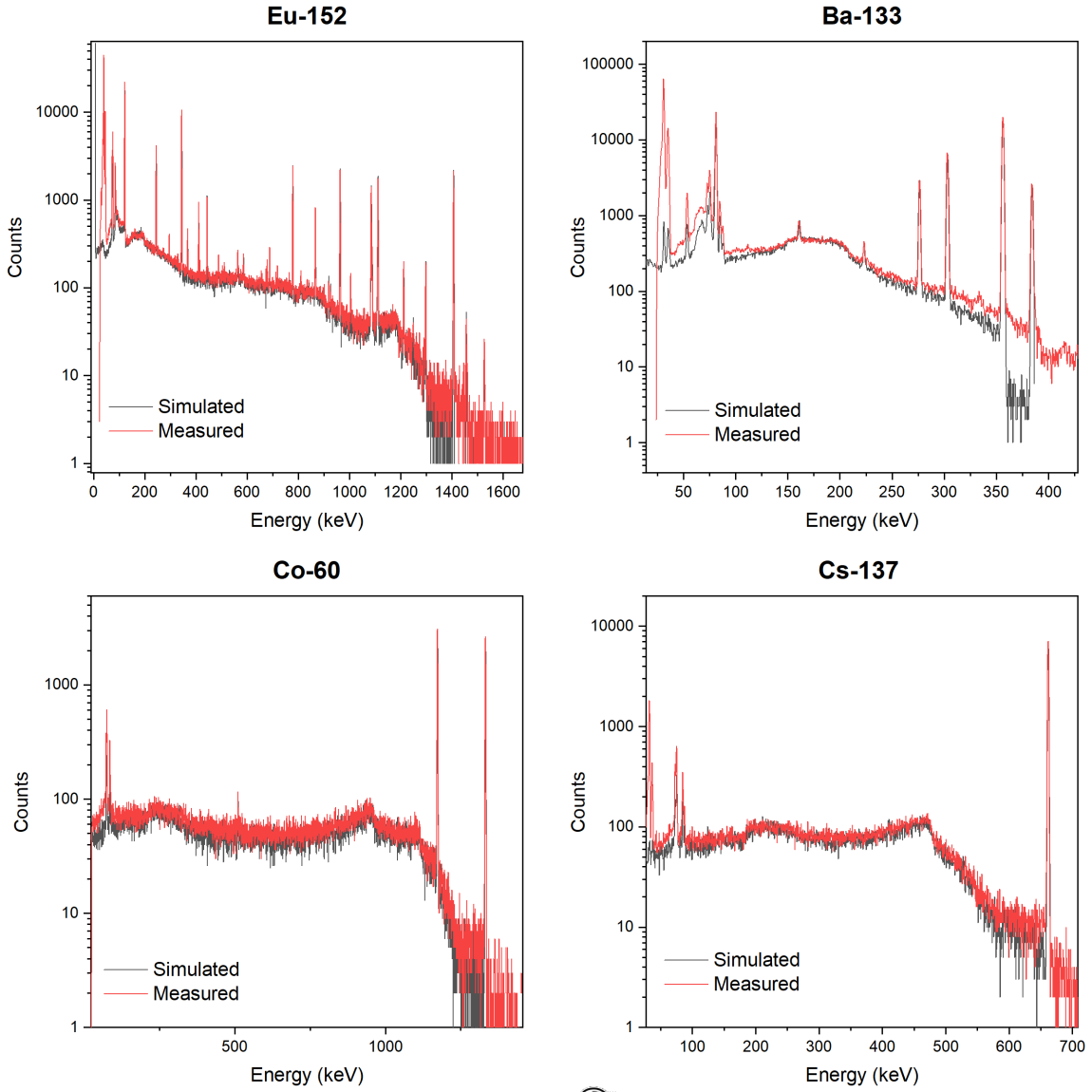

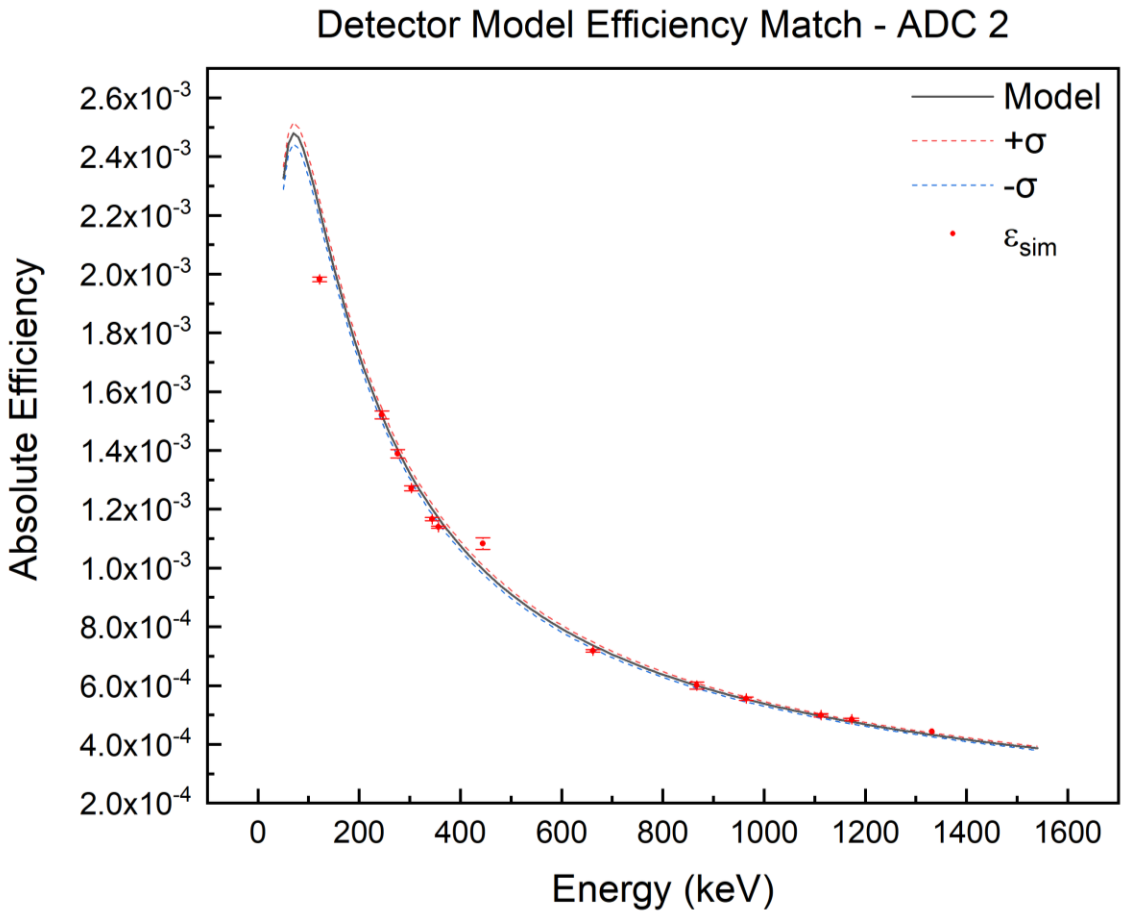

- Matched energy efficiency of model within 5%
- Foil vs. Point Source verification

Idaho National Laboratory

Oregon State University

Photofissions per pulse from photonuclear cross sections

- Need photofission event yield per pulse for absolute FPY calculations
- For ^{238}U photofission yield per pulse, the ratio of σ(γ,f)/σ(γ,n) and ^{237}U production from 208.0 keV γ-ray peak

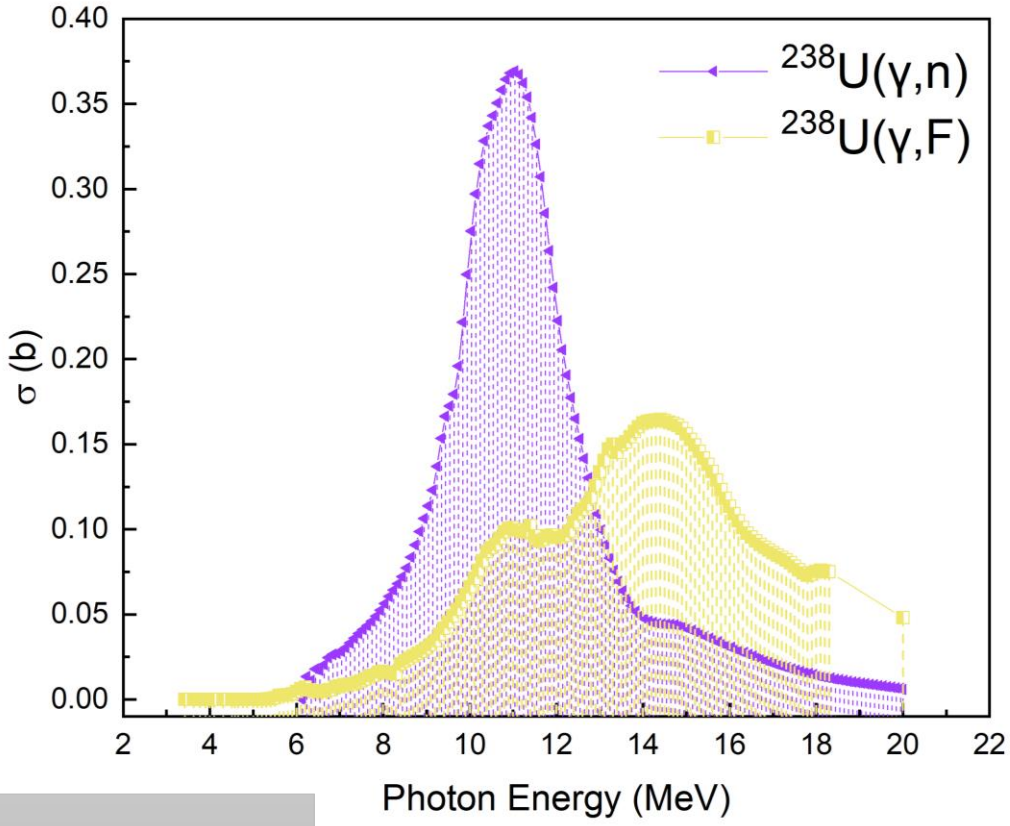

$$Y_{U238,f,pp} = \frac{\frac{C_{208}}{\beta \varepsilon A_p} \cdot \frac{RT}{LT}}{\sum_{M=0}^{cycles} \sum_{m=0}^{pulses} \int_{t_1}^{t_2} \sum_{i}^{M} e^{(-\lambda(T_M - T_i) + t + (m\tau)} \lambda \, dt} \cdot \frac{\int_0^B \frac{\phi(B,E)}{dE} \sigma_{U238,\gamma,f}(E) dE}{\int_0^B \frac{\phi(B,E)}{dE} \sigma_{U238\gamma,n}(E) dE}$$

[1] ENDF-B/VII.0: Accessed from Janis 4.0, Nuclear Energy Agency, Organization for Economic Co-operation and Development. https://www.oecd-nea.org/janis/

Photofissions per pulse from photonuclear cross sections

- Need photofission event yield per pulse for absolute FPY calculations
- For ^{232}Th photofission yield per pulse, the ratio of $\sigma_{U238}(\gamma,f)/\sigma_{Th232}(\gamma,f)$

$$Y_{Th232,f,pp} = Y_{U238,f,pp} \cdot \frac{\int_0^B \frac{\phi(B,E)}{dE}\sigma_{Th232,\gamma,f}(E)dE}{\int_0^B \frac{\phi(B,E)}{dE}\sigma_{U238,\gamma,f}(E)dE}$$

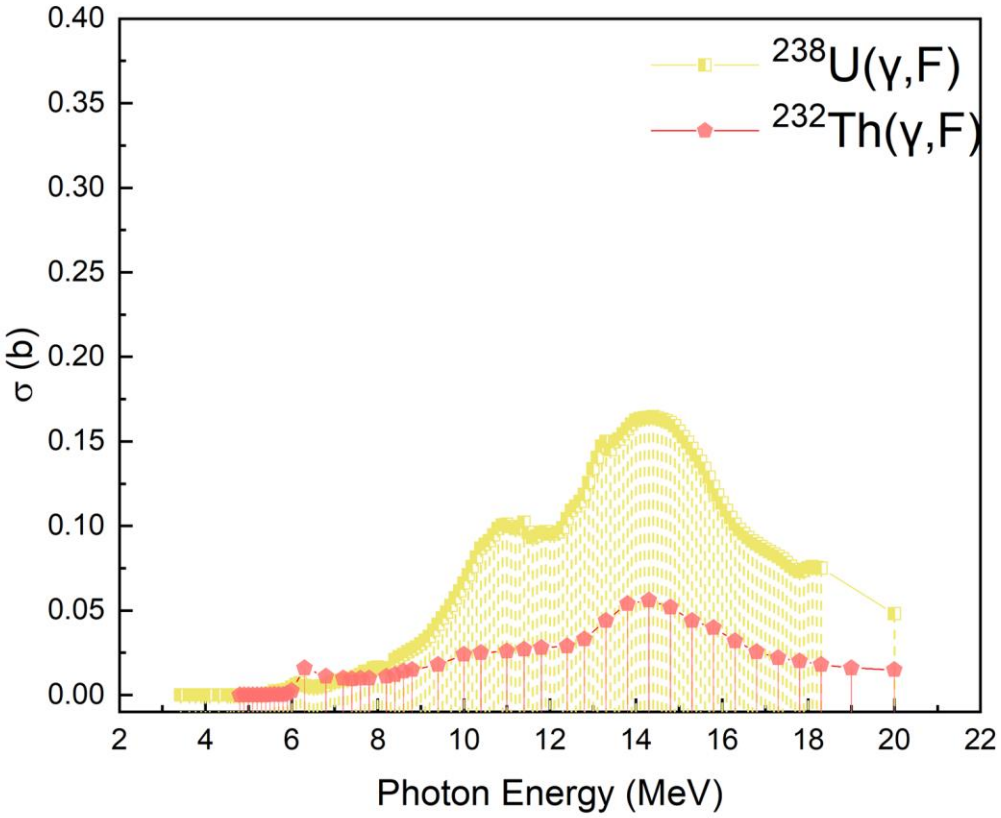

[1] ENDF-B/VII.0: Accessed from Janis 4.0, Nuclear Energy Agency, Organization for Economic Co-operation and Development. https://www.oecd-nea.org/janis/

3D Electron and Photon Beam

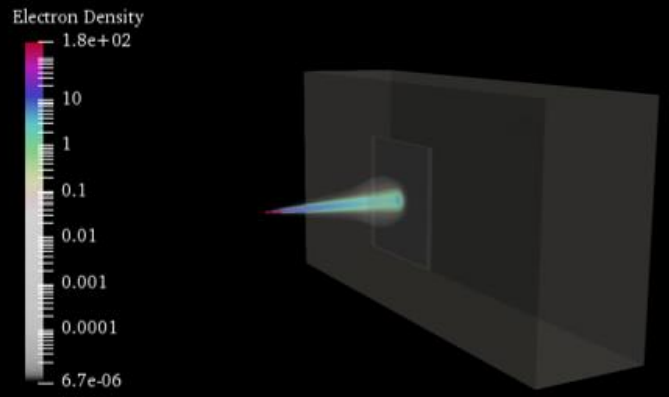

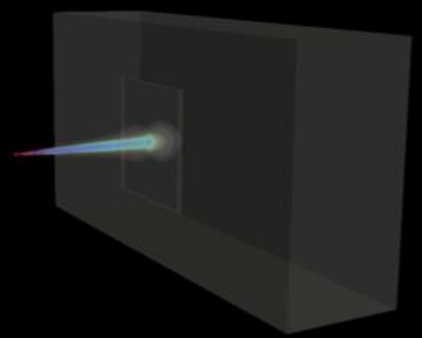

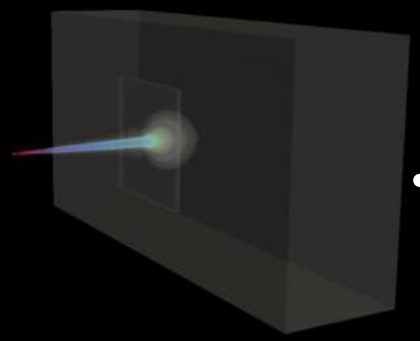

8 MeV

14 MeV

20 MeV

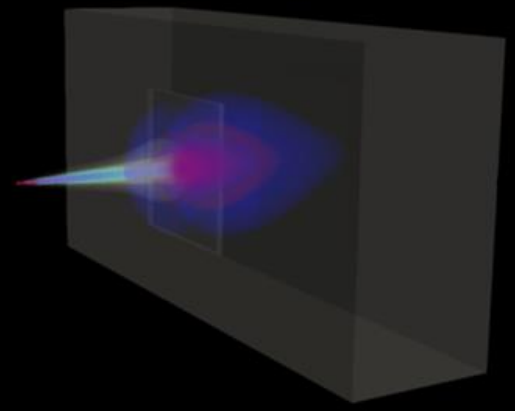

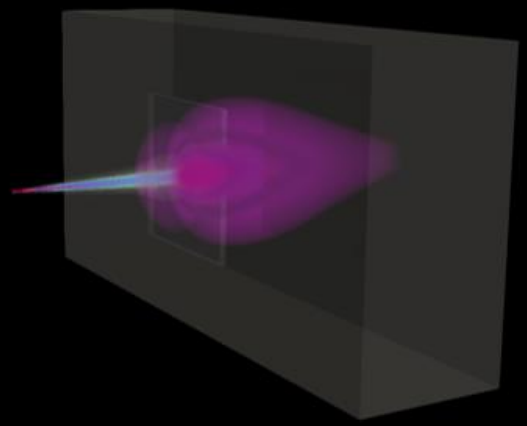

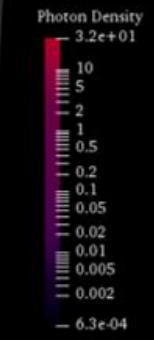

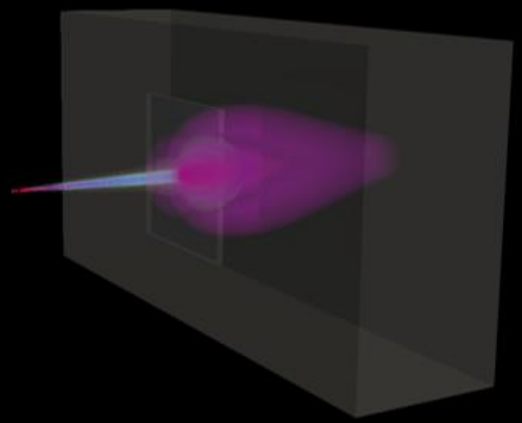

- MCNP6 3D mesh tally produced for electron and photon beam each E.E.
- Visualization of bremsstrahlung X-ray beam conversion

How is yield effected by an offset?

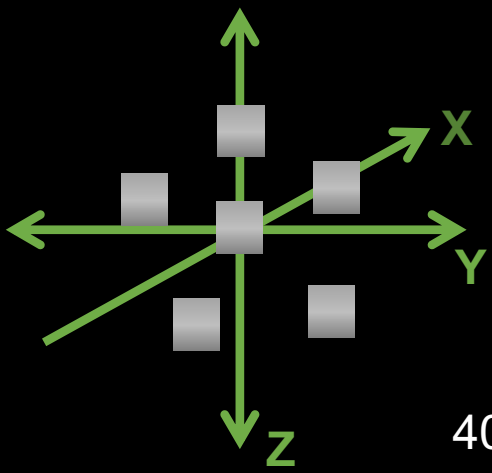

Uncertainty Contribution from Target Offset

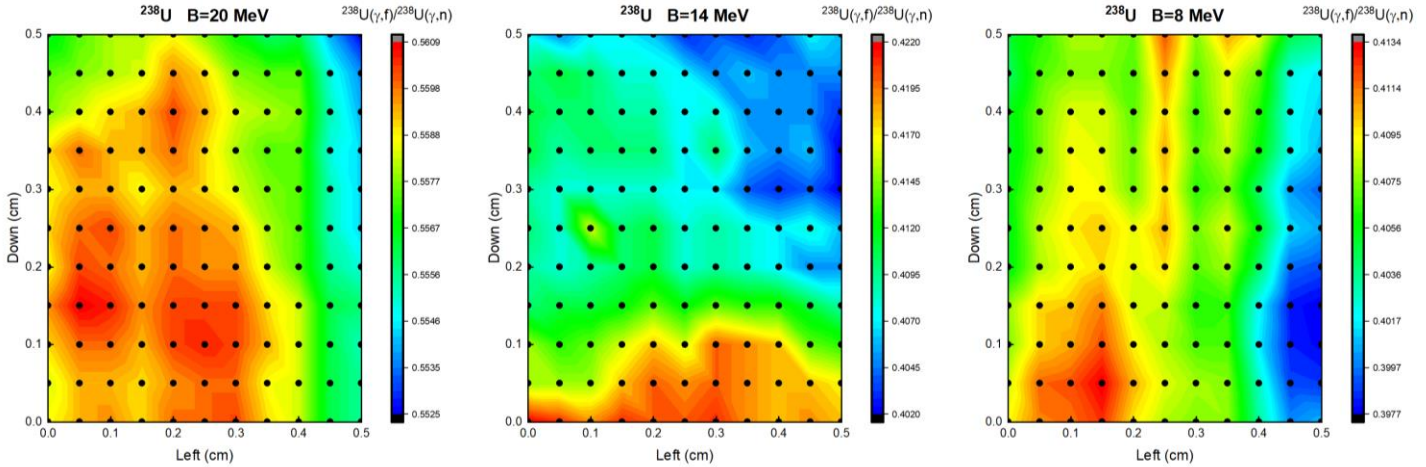

Ratio of ^{238}U photofission to ^{237}U production

$$R_{U238f} = \frac{\int_0^B \frac{\phi(B,E)}{dE}\sigma_{U238,\gamma,f}(E)dE}{\int_0^B \frac{\phi(B,E)}{dE}\sigma_{U238\gamma,n}(E)dE}$$

Ratio of ^{238}U photofission to ^{232}Th photofission

$$R_{Th238f} = \frac{\int_0^B \frac{\phi(B,E)}{dE}\sigma_{U238,\gamma,f}(E)dE}{\int_0^B \frac{\phi(B,E)}{dE}\sigma_{Th232,\gamma,f}(E)dE}$$

Uncertainty Contribution from Target Offset

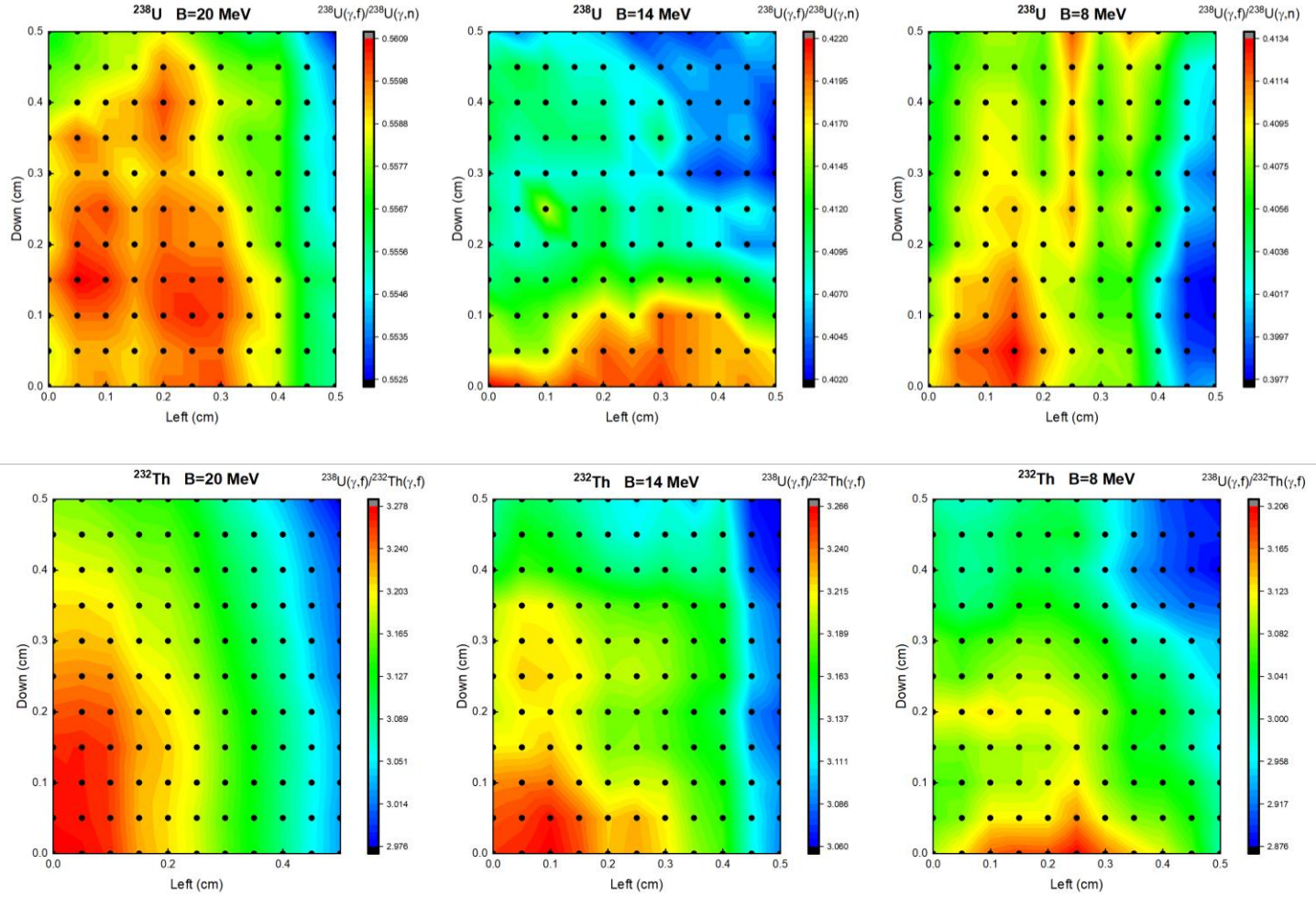

- 121 simulations for an offset of 0-0.5 cm in the left and down positions or each pair of target and endpoint energy
- Calculated incident beam energy ratio of cross sections
  - Photofission to ^{237}U production for uranium irradiations
  - Photofission of ^{238}U to ^{232}Th for thorium irradiations
- STD of sample taken as the conservative uncertainty of offset position during pneumatic transfer in calculating photofission events per pulse